

PROTEIN SEPARATION AND LABEL-FREE DETECTION  
ON SUPPORTED LIPID BILAYERS

A Dissertation

by

CHUNMING LIU

Submitted to the Office of Graduate Studies of  
Texas A&M University  
in partial fulfillment of the requirements for the degree of

DOCTOR OF PHILOSOPHY

August 2012

Major Subject: Chemistry

Protein Separation and Label-Free Detection on Supported Lipid Bilayers

Copyright 2012 Chunming Liu

PROTEIN SEPARATION AND LABEL-FREE DETECTION  
ON SUPPORTED LIPID BILAYERS

A Dissertation

by

CHUNMING LIU

Submitted to the Office of Graduate Studies of  
Texas A&M University  
in partial fulfillment of the requirements for the degree of

DOCTOR OF PHILOSOPHY

Approved by:

Chair of Committee,	Paul S. Cremer
Committee Members,	Siegfried M. Musser
	James D. Batteas
	Christian B. Hilty
Head of Department,	David H. Russell

August 2012

Major Subject: Chemistry

## ABSTRACT

Protein Separation and Label-Free Detection on Supported Lipid Bilayers. (August 2012)

Chunming Liu, B.S., Nanjing University

Chair of Advisory Committee: Dr. Paul S. Cremer

Membrane-bound proteins and charged lipids are separated based on their charge-to-size ratio by electrophoretic-electroosmotic focusing (EEF) method on supported lipid bilayers (SLBs). EEF uses opposing electrophoretic and electroosmotic forces to focus and separate proteins and lipids into narrow bands from an initially homogeneous mixture. Membrane-associated species were focused into specific positions within the SLB in a highly repeatable fashion. The steady-state focusing positions of the proteins could be predicted and controlled by tuning experimental conditions, such as buffer pH, ionic strength, electric field and temperature. Careful tuning of the variables should enable one to separate mixtures of membrane proteins with only subtle differences. The EEF technique was found to be an effective way to separate protein mixtures with low initial concentrations and it overcame diffusive peak broadening problem. A “SLB differentiation” post-separation SLB treatment method was also developed by using magnetic particles to rapidly slice the whole SLB into many small patches after electrophoretic separation, while keeping the majority of materials on surface and avoiding the use of chemical reactions.

Label-free detection techniques were also developed based on EEF on SLBs. First, a new separation based label-free detection method was developed based on the change of focusing position of fluorescently labeled ligands. This technique is capable of simultaneous detecting multiple protein competitive binding on the same ligand on SLBs. Low concentration protein can be detected in the presence of interfering proteins and high concentration of BSA. The fluorescent ligands were moved to different focusing positions in a charged SLB patch by different binding proteins. Both free ligand and protein bound ligand concentrations were obtained. Therefore, both protein identity and quantity information were obtained simultaneously. Second, the focusing position of fluorescent biomarkers on SLB was used to monitor the phospholipase D catalyzed hydrolysis of phosphatidylcholine (PC) to form phosphatidic acid (PA), which is involved with the change of charge on the phospholipids. The focusing position of fluorescent membrane-bound biomarker in the EEF experiment is directly determined by the negative charge density on SLB. Other enzyme reactions involved with the change of phospholipids charge can be monitored in a label-free fashion in a similar way.

## ACKNOWLEDGEMENTS

I would like to thank my committee chair, Dr. Cremer, and my committee members, Dr. Musser, Dr. Goodman, Dr. Batteas, and Dr. Hilty, for their guidance and support throughout the course of this research.

Thanks also go to my friends and colleagues and the department faculty and staff for making my time at Texas A&M University a great experience. I also want to extend my gratitude to the National Institute of Health, which provided the funding.

Finally, thanks to my mother and father for their encouragement.

## NOMENCLATURE

SLB	Supported Lipid Bilayer
SUV	Small Uni-lamellar Vesicle
FRAP	Fluorescence Recovery After Photobleaching
PDMS	Polydimethylsiloxane
EEF	Electrophoretic-Electroosmotic Focusing
PLD	Phospholipase D
StrA	Streptavidin
POPC	1-palmitoyl-2-oleoyl- <i>sn</i> -glycero-3-phosphocholine
POPA	1-palmitoyl-2-oleoyl- <i>sn</i> -glycero-3-phosphate
POPG	1-palmitoyl-2-oleoyl- <i>sn</i> -glycero-3-phospho-(1'- <i>rac</i> -glycerol)
NBD-DPPE	1,2-dipalmitoyl- <i>sn</i> -glycero-3-phosphoethanolamine- <i>N</i> -(7-nitro-2- 1,3-benzoxadiazol-4-yl)
TXR-DHPE	1,2-dihexadecanoyl- <i>sn</i> -glycero-3-phosphoethanolamine- <i>N</i> -Texas Red
NBDPE	1,2-dipalmitoyl- <i>sn</i> -glycero-3-phosphoethanolamine- <i>N</i> -(7-nitro-2- 1,3-benzoxadiazol-4-yl)

## TABLE OF CONTENTS

	Page
ABSTRACT .....	iii
ACKNOWLEDGEMENTS .....	v
NOMENCLATURE.....	vi
TABLE OF CONTENTS .....	vii
LIST OF FIGURES.....	ix
LIST OF TABLES .....	x
CHAPTER	
I INTRODUCTION.....	1
Cell Membrane and Supported Lipid Bilayer .....	1
Migration and Separation of Membrane-Associated Molecules on Supported Lipid Bilayers .....	2
Supported Lipid Bilayer Patterning and PDMS Stamping.....	5
Electrophoresis Flow Cell Device.....	7
II PROTEIN SEPARATION BY ELECTROPHORETIC- ELECTROOSMOTIC FOCUSING ON SUPPORTED LIPID BILAYER.....	9
Introduction .....	9
Experimental Section .....	11
Results .....	14
Discussion .....	23
Conclusions .....	32
III LABEL-FREE DETECTION OF COMPETITIVE BINDING ON SUPPORTED LIPID BILAYER .....	33
Introduction .....	33



CHAPTER		Page
	Experimental Section .....	36
	Results .....	40
	Discussion .....	53
	Conclusions .....	57
IV	LABEL-FREE DETECTION OF ENZYME REACTION ON SUPPORTED LIPID BILAYER IN SITU .....	59
	Introduction .....	59
	Experimental Section .....	63
	Results and Discussion.....	64
	Conclusions .....	72
V	COMPARTMENTALIZATION OF SUPPORTED LIPID BILAYER USING MAGNETIC PARTICLES.....	74
	Introduction .....	74
	Experiments and Results .....	76
	Conclusions .....	84
VI	CONCLUSIONS.....	86
	REFERENCES.....	88
	VITA .....	95

## LIST OF FIGURES

	Page
Figure 1 Electrophoretic Force and Electroosmotic Force .....	5
Figure 2 SLB Patterning Using PDMS Stamp .....	7
Figure 3 Flow Cell Device.....	8
Figure 4 Illustration of Electrophoretic-Electroosmotic Focusing .....	11
Figure 5 Migration of NBD-DPPE Lipids.....	15
Figure 6 Migration of Streptavidin .....	17
Figure 7 Schematic Diagram of Streptavidin Migration .....	18
Figure 8 Separation of Protein and Lipid Mixture.....	20
Figure 9 Electrophoretic-Electroosmotic Focusing of Individual Components .....	21
Figure 10 Calculation of Theoretical Focusing Positions.....	27
Figure 11 Effect of Buffer Ionic Strength.....	30
Figure 12 Effect of Negative Charge Density Gradient .....	31
Figure 13 Illustration of Label-Free Detection of Protein Competitive Binding .....	35
Figure 14 Synthesis of Biotin-cap-NBDPE .....	37
Figure 15 Focusing of Biotin-cap-NBDPE Lipids .....	41
Figure 16 Label-Free Detection of Goat Anti Biotin.....	43
Figure 17 Saturation Curve of Goat Anti Biotin .....	44
Figure 18 Limit of Detection of Goat Anti Biotin.....	45
Figure 19 Label-Free Detection of Streptavidin .....	46

Figure 20 Saturation Curve of Streptavidin.....	47
Figure 21 Simultaneous Detection of Streptavidin and Goat Anti Biotin.....	49
Figure 22 Label-Free Detection of Competitive Binding.....	51
Figure 23 Inhibition of Goat Anti Biotin Binding by Streptavidin .....	53
Figure 24 Detection of Streptavidin in Low Ionic Strength Condition .....	54
Figure 25 Effect of Surface Charge on Ligands Clustering .....	56
Figure 26 Detection in Narrower SLB.....	57
Figure 27 Illustration of Phospholipase D Catalyzed Lipid Hydrolysis.....	60
Figure 28 Schematic Diagram of Biomarker Focusing Position Change.....	62
Figure 29 Focusing of Biomarkers without Reaction.....	65
Figure 30 Focusing of Biomarkers in Different Conditions .....	68
Figure 31 Comparison of Biomarker Focusing Positions in Different Conditions ...	69
Figure 32 Migration Kinetics of Biomarkers in Different Conditions .....	70
Figure 33 Mass Spectrum of Phosphatidic Acid Product.....	71
Figure 34 Effect of Phosphatidic Acid on Biomarker Focusing Position .....	73
Figure 35 Compartmentalization of SLBs Using Magnetic Particles .....	76
Figure 36 Scratching SLBs Using Magnetic Particles .....	77
Figure 37 FRAP of SLBs with Different Amount of Scratches .....	79
Figure 38 Preservation of Separation Using Magnetic Particle Scratching .....	81
Figure 39 Preservation of Lipid and Protein Gradients.....	83
Figure 40 Relationship between Biotin-cap-NBDPE Fluorescent Intensity and Streptavidin Fluorescent Intensity.....	84

## LIST OF TABLES

	Page
Table 1 Charge, Radius and Zeta Potential of Proteins in the EEF Separation .....	23

## CHAPTER I

### INTRODUCTION

#### **Cell Membrane and Supported Lipid Bilayer**

Cell membranes are composed of the lipid bilayer structure with various kinds of membrane-associated proteins, such as integral proteins, trans-membrane proteins, peripheral proteins, and membrane bound proteins. The cell membrane separates the interior of cells from the outside environment and controls the movement of substances into and out of cells. It is also involved in cell signaling processes and bio-synthetic reactions. The study of individual proteins or reactions is limited by the complexity of cell membranes. Therefore, supported lipid bilayer (SLB) model systems are widely used in the study of protein-membrane and membrane-membrane interactions,<sup>1-4</sup> biophysical properties of different types of lipids,<sup>5</sup> lateral mobility of biomolecules<sup>6</sup> and so on. Lipid molecules are amphiphilic, with hydrophobic acyl chains and hydrophilic head groups. In aqueous solution, lipid molecules will form micelles or bilayer vesicles to avoid the exposure of hydrophobic acyl chains to the aqueous solution. SLBs have been formed on different types of solid supports, such as quartz, mica, glass, PDMS, gold and titanium oxide.<sup>7-11</sup> There are two major procedures to form SLBs. One is vesicle fusion, where a high concentration of lipid vesicles is incubated on the solid support. Vesicles will adsorb on solid support and fuse to form larger vesicles, and

---

This dissertation follows the style of *Analytical Chemistry*.

finally rupture to form the SLB. The other method is using layer by layer deposition on a hydrophilic surface using Langmuir-Blodgett. Between the lipid bilayer and the solid support surface, there is a 1-2 nm thick water layer that prevents the direct contact between the SLB and the solid support.

SLBs have several advantages over black lipid membrane or suspended lipid membranes. One of the greatest advantages of the SLB is its stability. SLBs can remain stable under conditions of mechanical flow and vibrations, and an electric field parallel to the SLB surface.<sup>4,12-14</sup> Unlike suspended lipid membranes, the presence of holes will not destroy the entire bilayer. Because of this stability, experiments lasting days or weeks are possible with a SLB while suspended lipid bilayer experiments are usually limited to hours.<sup>15</sup> Another advantage of the supported bilayer is that, it is accessible to a number of characterization techniques, such as atomic force microscope (AFM), surface plasma resonance (SPR) and quartz crystal microbalance (QCM), which would be impossible on a freely floating sample.

### **Migration and Separation of Membrane-Associated Molecules on Supported Lipid Bilayers**

In lipid membranes, lipids have high lateral mobility in the plane of the bilayer when the temperature is higher than the gel-liquid phase transition temperature. Fluorescence recovery after photobleaching (FRAP) is a method commonly used to determine lipid mobility. In FRAP experiments, fluorescently labeled lipids mixed with

other lipids are bleached by strong illumination in a small area of the lipid bilayer. Due to the lateral diffusion of lipids, the bleached fluorescently labeled lipids diffuse out of the bleached area and fluorescently labeled lipids diffuse into the bleached area. Therefore, the fluorescent intensity of the bleached area recovers with the increase of time. Membrane-associated proteins were also found to have the lateral mobility by FRAP experiments.

Other than free diffusion, the controlled migrations of lipids and proteins have been realized on SLBs using an electric field. In 1977, Poo et al. found that Concanavalin A, a carbohydrate-binding protein, was moved by an external electric field and accumulated on muscle cell membrane.<sup>16</sup> Later on, the migration of membrane-bound protein and lipids by an electric field was also achieved on SLBs.<sup>17,18</sup> Membrane anchored proteins with alpha-helical hydrophobic membrane-embedded regions could also migrate and be concentrated by an electric field on SLBs.<sup>19</sup> A theoretical model for protein migration on SLB was also developed.<sup>20</sup> With the addition of an external electric field parallel to SLB planar surface, membrane-associated species were affected by electrophoretic force and electroosmotic force (**Figure 1**). Electrophoretic force was generated by the charges on the membrane-associated species. Electroosmotic force was generated by the migration of counter-ions that were attracted by the surface charges on lipid bilayers in electric field. For negatively charged lipid bilayers and negatively charged membrane-associated species, the electrophoretic force has opposite direction to the electroosmotic force. When membrane-associated species migrate in a lipid bilayer, there is also a friction force on the opposite direction of migration.

This theory provided clues for the realization of biomolecule separation on SLBs. The first separation on SLB was achieved by the difference in migration velocities of different lipids in an electric field.<sup>12</sup> The separation matrix SLB was formed by vesicle fusion on glass slide. Then a narrow line of separation matrix SLB was removed by scratching, and vesicles containing the analytes were used to back fill the scratch and form a SLB. Then the analytes started to migrate from a narrow line and finally were separated after migrating for a long enough distance. Because lipids molecules in SLBs did not experience strong electroosmotic force, the separation was mainly based on the difference in electrophoretic force and friction force on different lipids. In this dissertation, electrophoretic force and electroosmotic force will be used to focus and separate membrane-bound proteins from homogeneous mixtures on SLBs. The friction force will not appear in the focusing separation, because finally the migration velocities of membrane-bound proteins are zero.



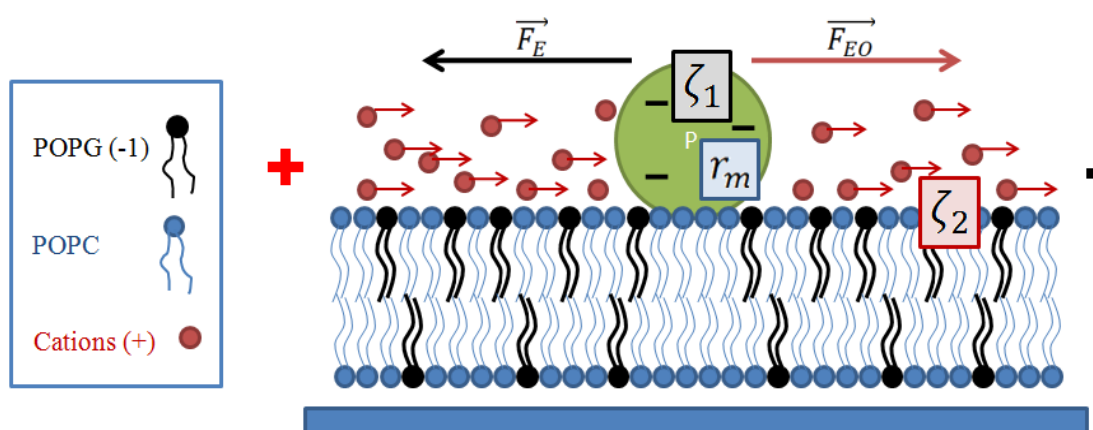


**Figure 1.** Electrophoretic Force and Electroosmotic Force. The picture is an illustration of electrophoretic force and electroosmotic force on negatively charged proteins bound on negatively charged SLB surface. Electrophoretic force is generated by the negative charges on protein. Electroosmotic force is given by the electroosmotic flow generated by the migration of cations near negatively charged surface. In this particular situation, the electrophoretic force and electroosmotic force on the protein are in opposite directions.

### Supported Lipid Bilayer Patterning and PDMS Stamping

SLBs can be patterned on a surface in order to produce multiple isolated regions on the same substrate. SLB patterns were produced using mechanical scratches or physical barriers formed by metals or proteins to prevent mixing between adjacent SLB patches while still allowing free diffusion of lipids and proteins within each SLB patch. In the past, several methods have been developed to produce well patterned SLBs, such as the removal and stamping of lipid bilayer using PDMS stamps, UV radiation

photolithography, AFM (Atomic Force Microscope) patterning and so on.<sup>10,21-28</sup> In all experiments, strong physical barriers are needed to confine the migration of lipids and proteins on SLB surface, thus SLB patches have to be made in a simple and highly repeatable way.

Herein, SLB patches were produced following the PDMS stamping procedure. PDMS monomer and cross-linker were mixed in a 10:1 mass ratio. The mixture was stirred and vacuum degassed. PDMS was then poured over a patterned glass mold and cured at room temperature overnight. The glass master consisted of a series of ten 380  $\mu\text{m}$  wide parallel lines that were 1 cm long and separated from one another by 200  $\mu\text{m}$  spacers. The glass master was prepared using photolithography followed by standard HF etching technique.<sup>4</sup> The PDMS stamp was carefully peeled away from the glass, washed with ethanol, and rinsed with purified water. In all experiments performed herein, each SLB patch was about 380  $\mu\text{m}$  wide and isolated from the adjacent region by a fibrinogen monolayer adsorbed onto the planar glass substrate. To form SLB patches, a PDMS stamp was placed on a clean cover glass slide. 1.0 mg/mL fibrinogen solution (in 10mM PBS buffer) was added to form a fibrinogen monolayer on the exposed glass area. After 1 hour incubation, the fibrinogen was rinsed away with 10 mM Tris buffer, and the PDMS stamp was removed. Finally, 1 mg/mL lipid vesicle solution was introduced and SLBs formed spontaneously on the area without the fibrinogen monolayer (**Figure 2**).<sup>27</sup>

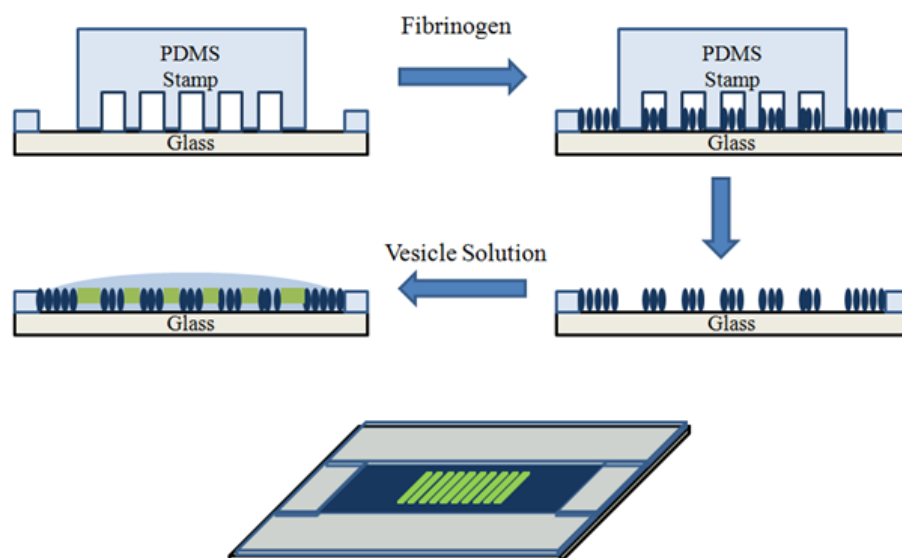


**Figure 2.** SLB Patterning Using PDMS Stamp.<sup>14</sup> Patterned SLBs were formed on glass. Each SLB patch was about 380  $\mu\text{m}$  wide and isolated from the adjacent region by a fibrinogen monolayer adsorbed to the planar glass substrate.

### Electrophoresis Flow Cell Device

In electrophoresis experiments on SLBs, an external electric potential is needed to provide the driving force for charge migration. In the following experiments, over 100 Volts was used. This voltage is so high that it can electrolyze water and generates protons and oxygen gas at the anode and hydroxide anions and hydrogen gas at the cathode. Although electrophoresis is run in buffered solution, the buffer solution has to be constantly changed to maintain the pH value on SLB surface. Gas bubble generated on the electrodes can also destroy SLB. Also, Joule heating during electrophoresis is another problem that can impair the separation results and the stability of SLB structure.

In order to get rid of the electrolyzed gas bubbles and maintain the pH and temperature in electrophoresis experiments, the electrophoresis experiments on SLBs were conducted in a flow cell device (**Figure 3**).<sup>29</sup> In this device, two buffer flows are used to continuously flush each electrode, and the majority of electrolyzed products are flushed out. Because the electrophoresis experiments on SLBs take more than 30 minutes, to ensure the removal all electrolyzed product, two extra inner buffer flows are added. The pH of the electrophoresis buffer can be controlled within 0.2 pH units.<sup>29</sup> This device also enable the used of high ionic strength solutions in electrophoresis experiments at higher buffer flow rates.

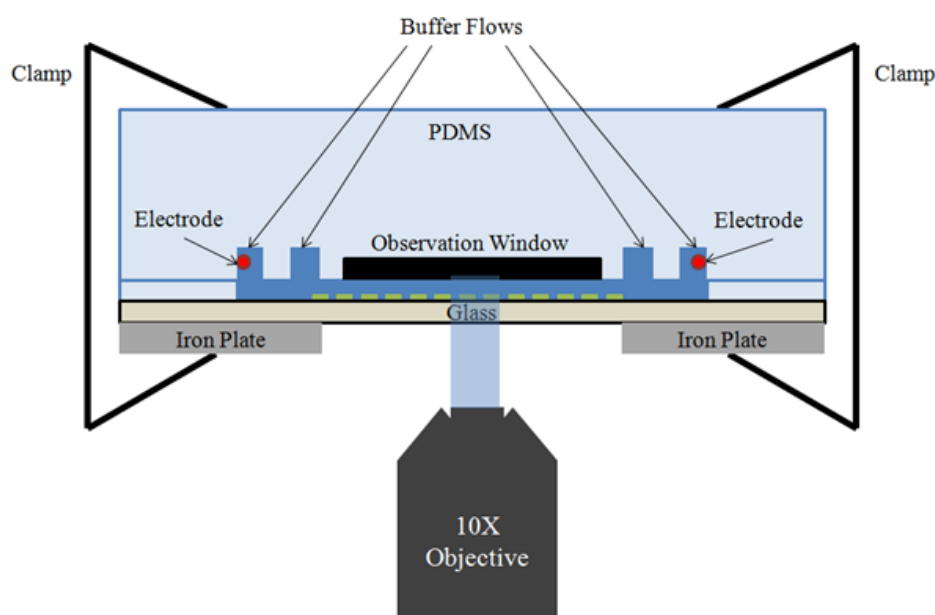


**Figure 3.** Flow Cell Device.<sup>14</sup> The distance between the two electrodes is 2 cm and the length of the observation window is 1 cm. The distance between the top of the bottom glass slide and bottom of the observation window is about 100  $\mu\text{m}$ . The SLB is coated on the lower glass slide. The drawing is not to scale.

CHAPTER II  
PROTEIN SEPARATION BY ELECTROPHORETIC-ELECTROOSMOTIC  
FOCUSING ON SUPPORTED LIPID BILAYER\*

**Introduction**

The extraction and separation of membrane proteins from cells has traditionally involved the use of detergents and sonication. This method, however, can destroy the native structures, oligomerization states and activities of membrane proteins. This has led to a search for new methods for separating membrane proteins within supported lipid bilayer (SLB) environments, which should help preserve protein structure and activity.<sup>30-</sup>

33

Separation experiments in supported bilayers have been performed by laminar flow, surface acoustic wave, and electrophoresis methods.<sup>9,13,34,35</sup> Electrophoretic techniques, pioneered by Sackmann,<sup>36</sup> have been used to manipulate fluorescently labeled lipids, membrane-bound proteins and tethered lipid vesicles on SLBs.<sup>8,12,17,18,24,37-39</sup> For example, electrophoresis and electroosmosis have been employed to manipulate the migration of membrane-associated species in patterned SLB patches.<sup>8,18,38,39</sup> However, the separation of multiple components has been challenging.

---

\* Reprinted with permission from “Protein Separation by Electrophoretic-Electroosmotic Focusing on Supported Lipid Bilayers” by Liu, C.; Monson, C. F.; Yang, T.; Pace, H.; Cremer, P. S., 2011. *Anal. Chem.*, 83, 7876. Copyright 2012 by American Chemical Society.

Several charged lipids were separated in SLBs with a method similar to gel electrophoresis.<sup>12</sup> The lipids were separated based on their drift velocities in the electric field, which depended in part on the specific interactions between the analytes and the SLB matrix. Unfortunately, sample loading difficulties as well as peak broadening reduced the wide application of this method.

Herein, we report a novel method, EEF, for bilayer species separation inspired by the isoelectric focusing technique.<sup>40</sup> EEF uses the electrophoretic force and an opposing electroosmotic gradient to focus negatively charged membrane-associated proteins and lipids from an entire SLB patch into narrow bands. The more negatively charged the molecule, the closer it will focus to the positive electrode, due to the larger electrophoretic contribution. However, the larger the molecule's cross section within the aqueous solution, the closer the focusing position will be to the negative electrode, due to the electroosmotic contribution. The steady state position of a given molecule results from the combination of these two physical characteristics, as illustrated in **Figure 4**. The EEF technique was found to be an effective way to separate protein mixtures with low initial concentrations, and it overcame diffusive peak broadening to allow many bands to be separated simultaneously within a single membrane.

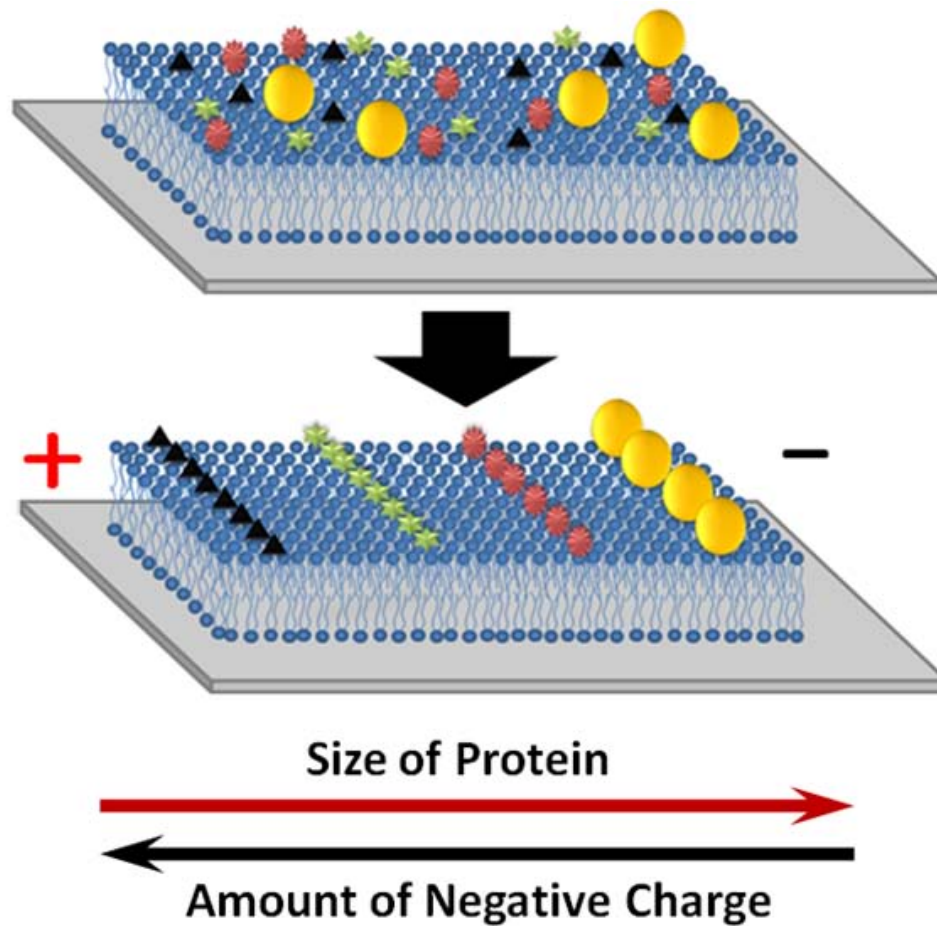


**Figure 4.** Illustration of Electrophoretic-Electroosmotic Focusing. In EEF, an applied electric field focuses membrane-bound species from an initial disordered state (top) into bands (bottom). The focusing position depends on the size and charge of the species.

## Experimental Section

### Materials

Fibrinogen, streptavidin and anti-biotin IgG were purchased from Sigma (St. Louis, MO). The latter two proteins were labeled according to procedures described

previously.<sup>29</sup> 1-palmitoyl-2-oleoyl-*sn*-glycero-3-phosphocholine (POPC), 1-palmitoyl-2-oleoyl-*sn*-glycero-3-phospho-(1'-*rac*-glycerol) (POPG), 1,2-dioleoyl-*sn*-glycero-3-phosphoethanolamine-*N*-(cap biotinyl) (biotin-cap-DOPE), and 1,2-dipalmitoyl-*sn*-glycero-3-phosphoethanolamine-*N*-(7-nitro-2-1,3-benzoxadiazol-4-yl) (NBD-DPPE) were purchased from Avanti Polar Lipids (Alabaster, AL). Polydimethylsiloxane (PDMS) was obtained from Dow Corning (Sylgard, silicone elastomer-184).

### SLB Formation

SLBs were formed by the vesicle fusion method<sup>7,21</sup> on clean glass coverslips (Corning, NY, 22×22 mm, No. 2). The coverslips were cleaned in a boiling 1:3 solution of 7X detergent (MP Biomedicals, Solon, OH) and purified water. Purified water came from an Ultrapure Water System (Thermo Scientific Barnstead Nanopure Life Science, Marietta, OH). The coverslips were rinsed with copious amounts of this water, dried with nitrogen, and annealed in a kiln at 500 °C for 5 h before use. Small uni-lamellar vesicles (SUVs) with 10% POPG, 0.5% NBD-DPPE, 1% biotin-cap-DOPE and 88.5% POPC were prepared by vesicle extrusion. To do this, the lipids were mixed in chloroform. The chloroform was subsequently evaporated under a stream of nitrogen followed by vacuum desiccation for 4 h. Then the lipids were rehydrated in phosphate buffered saline (PBS) solution which consisted of 10 mM sodium phosphate, 150 mM NaCl, and 0.2 mM sodium azide. The pH of the PBS solution was tuned to 7.4 with a small amount of 1M HCl. The total concentration of the lipids in solution was 1.0



mg/mL. After several freeze-thaw cycles, the solutions were extruded through a polycarbonate filter (Whatman) with 100 nm pores.

#### PDMS Stamp and SLB Patterning

PDMS monomer and cross-linker were mixed in a 10:1 mass ratio. The mixture was stirred and vacuum degassed. PDMS was then poured over a patterned glass mold and cured at room temperature overnight. The glass master consisted of a series of ten 380  $\mu\text{m}$  wide parallel lines that were 1 cm long and separated from one another by 200  $\mu\text{m}$  spacers. The glass master was prepared using standard HF etching techniques described previously.<sup>4</sup> The PDMS stamp was carefully peeled away from the glass, washed with ethanol, and rinsed with purified water. In all experiments performed herein, each SLB patch was about 380  $\mu\text{m}$  wide and isolated from the adjacent region by a fibrinogen monolayer adsorbed onto the planar glass substrate. To form SLB patches, a PDMS stamp was placed on a clean cover glass slide. 1.0 mg/mL fibrinogen solution (in 10mM PBS buffer) was added to form a fibrinogen monolayer on the exposed glass area. After a 1 hour incubation, the fibrinogen was rinsed away with 10 mM Tris buffer, and the PDMS stamp was removed. Finally, 1 mg/mL lipid vesicle solution was introduced and SLBs formed spontaneously on the area without the fibrinogen monolayer (**Figure 2**).<sup>27</sup>

## Fluorescence Imaging and Flow Cell

Epifluorescence images were obtained using a Nikon E800 fluorescence microscope with a Roper Scientific MicroMAX 1024B charge-coupled device (CCD) camera (Princeton Instruments). A flow cell described previously<sup>29</sup> was used to constantly control the pH and ionic strength over the course of an EEF experiment (**Figure 3**). All experiments were performed with a 10 mM pH 7.3 Tris buffer. The buffer was flowed through the channels at a rate of 25 mL/hour per channel.

## Results

In a first experiment, the migration of negatively charged fluorescent lipids NBD-DPPE was observed as a function of time at an applied field of 50 V/cm. (**Figure 5**). As can be seen, NBD-DPPE, which is negatively charged at pH 7.3, was pushed toward the positive electrode (left) by the electrophoretic force in the beginning. Although the SLB contained 10 % negatively charged POPG lipids, which should also migrate towards the positive electrode (left) by the electrophoretic force, the migration of NBD-DPPE was not apparently affected by the migration of POPG lipids. Actually, NBD has a small portion of negative charge at pH 7.3. Thus NBD-DPPE has more negative charge than POPG, so that NBD-DPPE felt stronger electrophoretic force and should move faster than POPG. As shown in **Figure 5**, NBD-DPPE lipids continued building up on the positive electrode side of the SLB, and finally concentrated into a single peak.

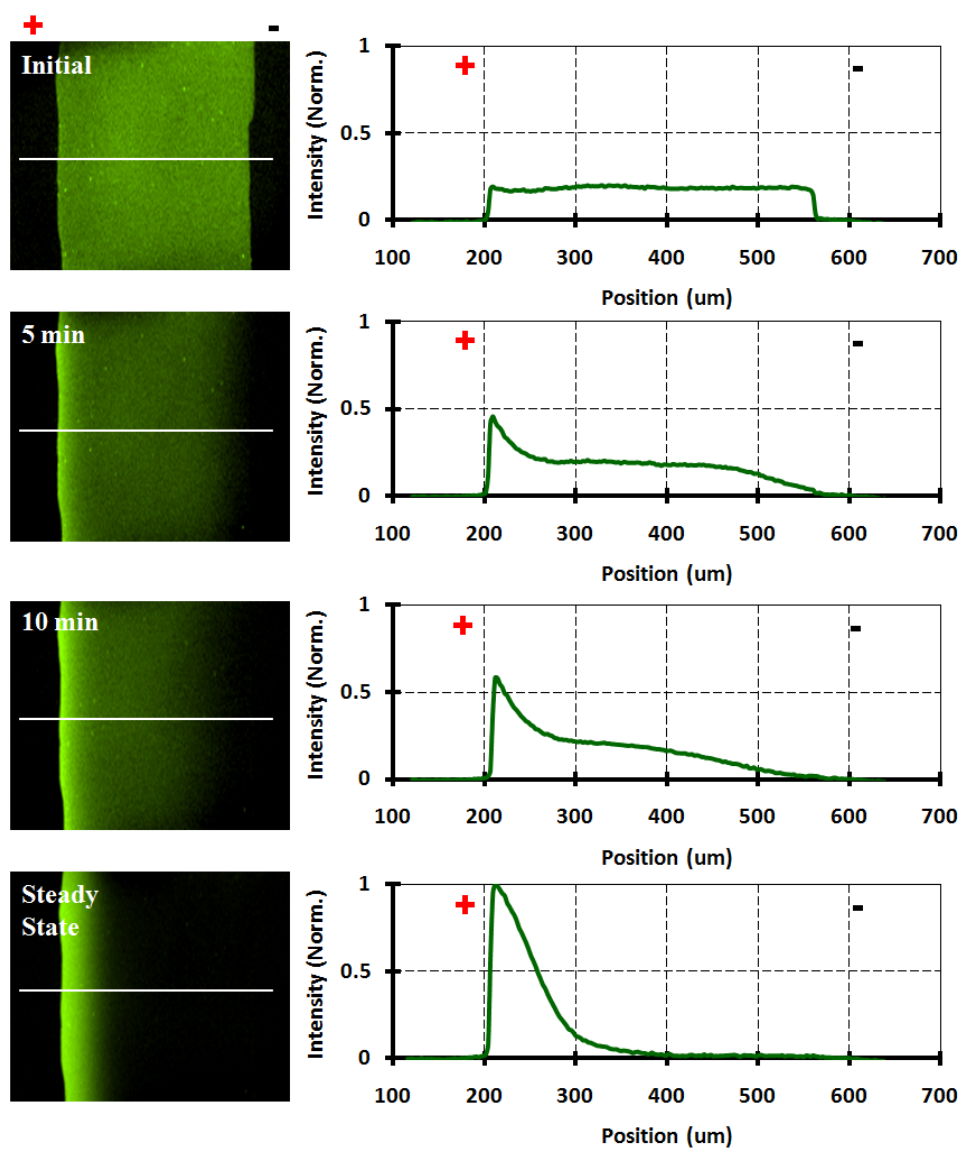


**Figure 5.** Migration of NBD-DPPE Lipids. NBD-DPPE lipids were moved by 50 V/cm electric field in negatively charged lipid bilayer (10% POPG). pH was 7.3, controlled by 10mM Tris buffer. The corresponding line-scan profile is on the right of each image.

Streptavidin with four Alexa-488 dyes per molecule (StrA-4) was attached to the bilayer. This was done by incubating a 5 nM StrA-4 solution over the membrane containing 1% biotin-cap-DOPE for 30 min. followed by the rinsing away of excess protein. The membrane attached proteins were observed as a function of time at an applied field of 50 V/cm. (**Figure 6**). As can be seen, the streptavidin, which is negatively charged at pH 7.3, was pushed toward the negative electrode (right) by the electroosmotic force in the first five minutes. However, it changed directions after 10 min and ultimately accumulated in a narrow band between the anodic edge and the middle of the patch. The origin of this behavior lies with the negatively charged POPG molecules, which move anodically (left) to form a gradient starting from the extreme left edge of the patch.<sup>17</sup> Initially, the POPG was uniformly distributed and, hence, the electroosmotic contribution was initially uniform over the entire patch, which caused the streptavidin to move to the right. Once the POPG gradient was established, however, the streptavidin moved electrophoretically to the left until the counterforce from the electroosmotic gradient exactly matched the electrophoretic contribution (**Figure 7**). It should be noted that there are a few immobile bright spots in the micrograph. They are probably two dimensional protein crystallites or aggregates that can form on lipid bilayers under the appropriate pH and ionic strength conditions.<sup>3,41,42</sup>

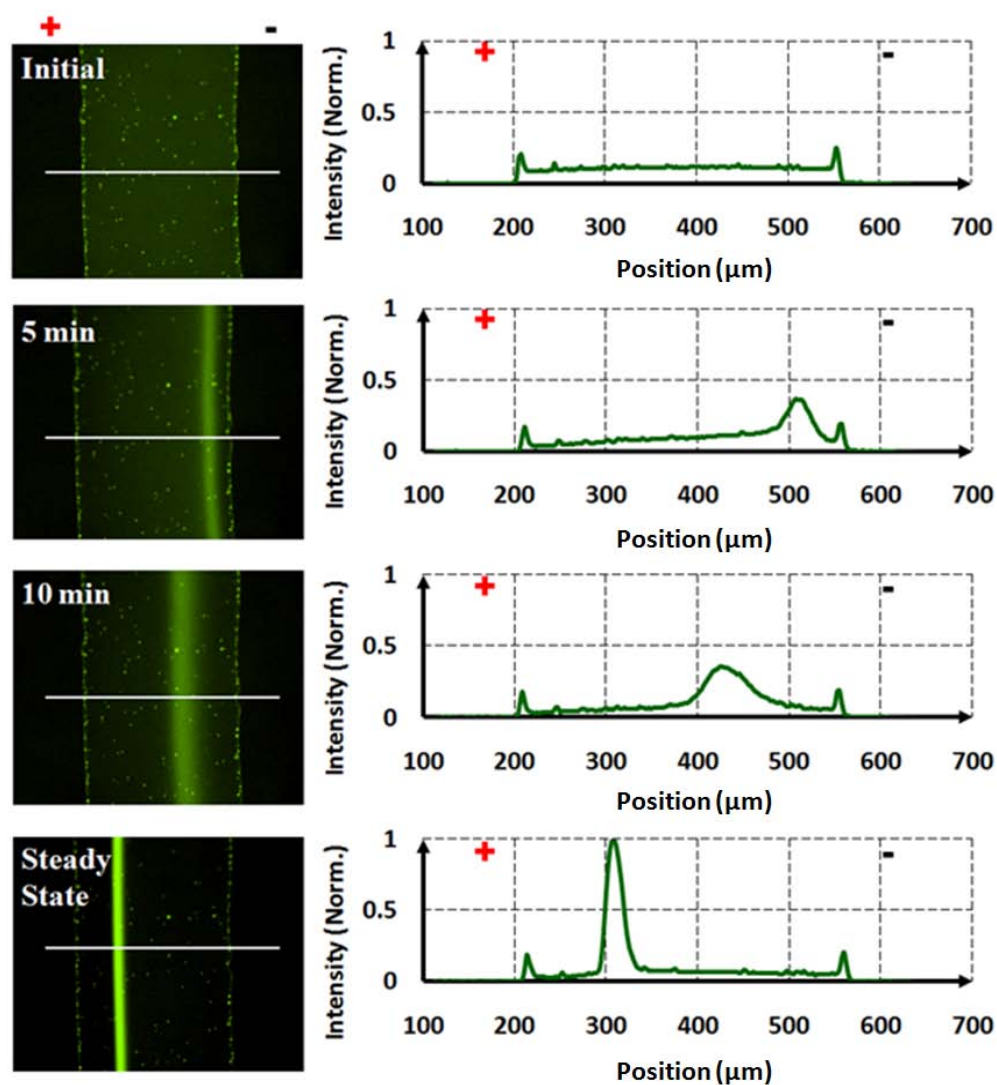


**Figure 6.** Migration of Streptavidin. The pictures shows the migration of StrA-4 in a lipid bilayer containing 10 mol% POPG and 1% biotin-cap-DOPE with a 50V/cm applied electric field. The pH was 7.3 and controlled by using 10 mM Tris buffer. The corresponding line scan profile is to the right of each image. The very small peaks along the edges were immobile proteins along the patch boundaries.

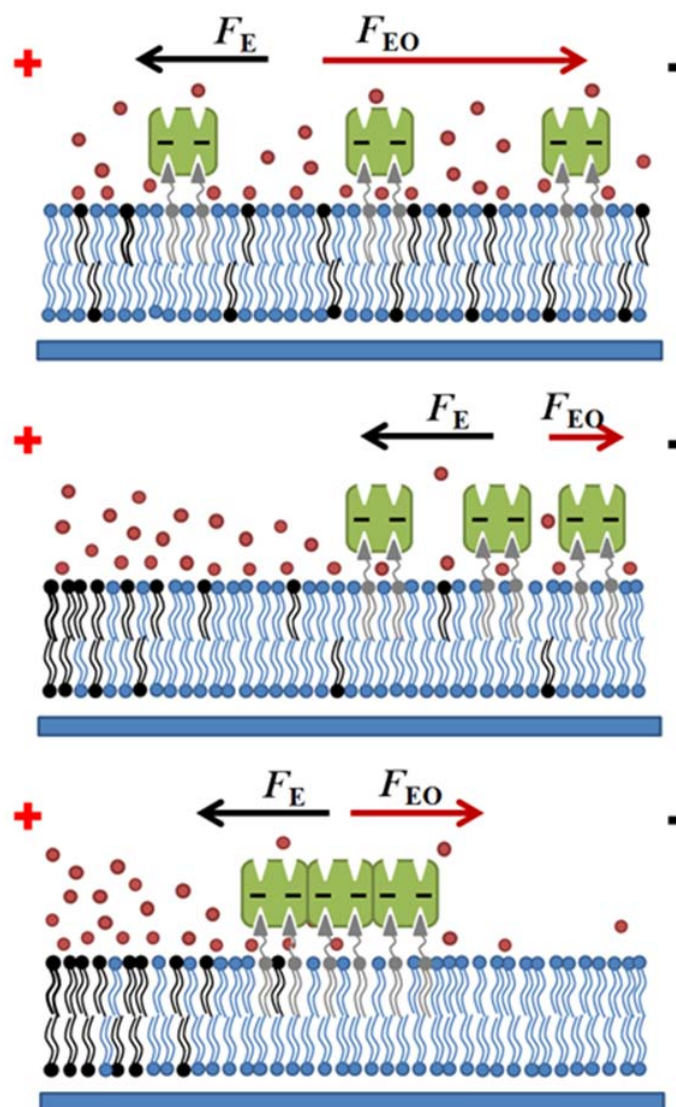


**Figure 7.** Schematic Diagram of Streptavidin Migration.  $F_E$  is the electrophoretic force, and  $F_{EO}$  is electroosmotic contribution.

Multiple proteins could be separated from one another and concentrated by exploiting the EFF method. This is demonstrated experimentally in **Figure 8**, where a negatively charged fluorescent lipid (NBD-DPPE), anti-biotin IgG (labeled with two Alexa-594 per molecule), StrA-1 (Streptavidin labeled with one Alexa-488 dyes per molecule) and StrA-4 were separated in the same SLB. After the SLB containing 10 % POPG, 1% biotin-cap-DOPE, 0.5 % NBD-DPPE and 88.5 % POPC was prepared, the three proteins were pre-mixed in solution (5 nM for StrA-1 and StrA-4 and 50 nM for the IgG) and incubated above it for 30 minutes. Excess protein molecules were washed away before fluorescence imaging. As can be seen, the protein concentration was initially uniform across the entire bilayer. However, after applying a 50 V/cm electric field for one hour, the individual components migrated to their specific focusing positions. EFF experiments were also done separately on each membrane-bound protein with NBD-DPPE lipids on the same kind of SLB (**Figure 9**). In both separated experiments (**Figure 9**) and the mixed experiment (**Figure 8**), the same kind of component has identical focusing position. Therefore, the focusing position could be used to determine the identity of the protein, on the same SLB and experimental conditions.

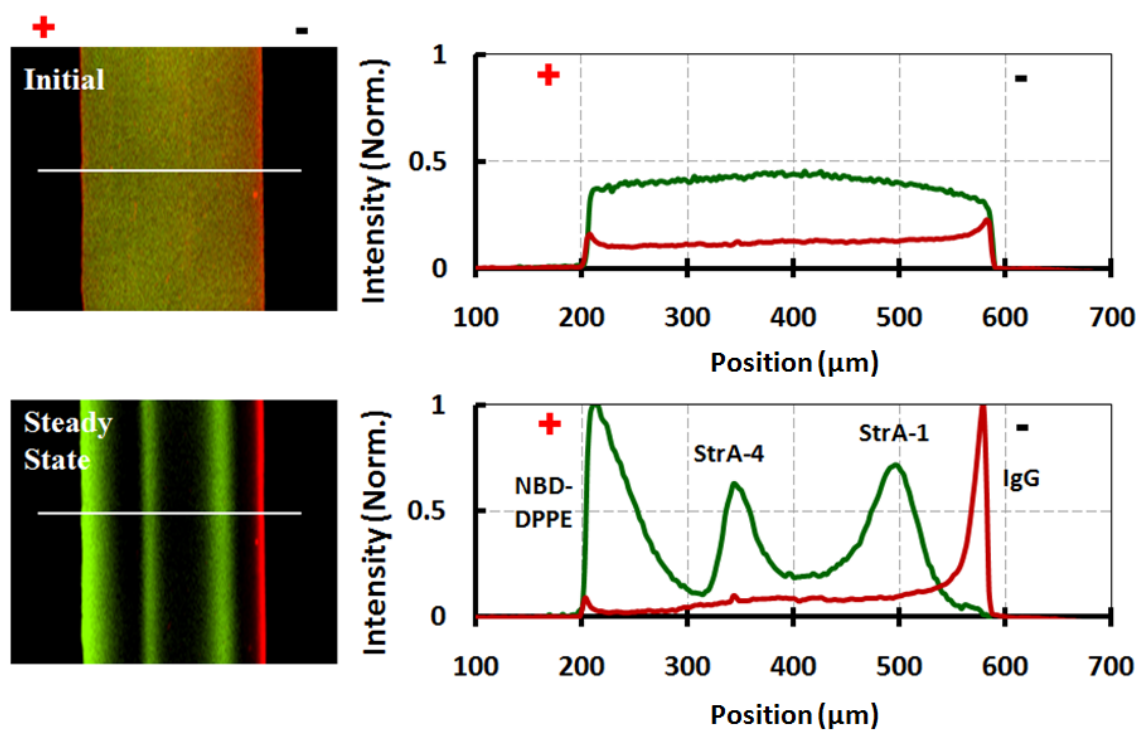


**Figure 8.** Separation of Protein and Lipid Mixture. Proteins and fluorescent lipids mixture were separated in a SLB containing 10 mol% POPG. The solution was a 10 mM Tris buffer at pH 7.3. The top image shows the membrane before the field was applied. The bottom image was taken after the application of a 50 V/cm potential for 30 min. Adjacent to each image is the corresponding fluorescent line scan profile. The bands on the bottom image from left to right are NBD-DPPE, StrA-4, StrA-1 and anti-biotin IgG.



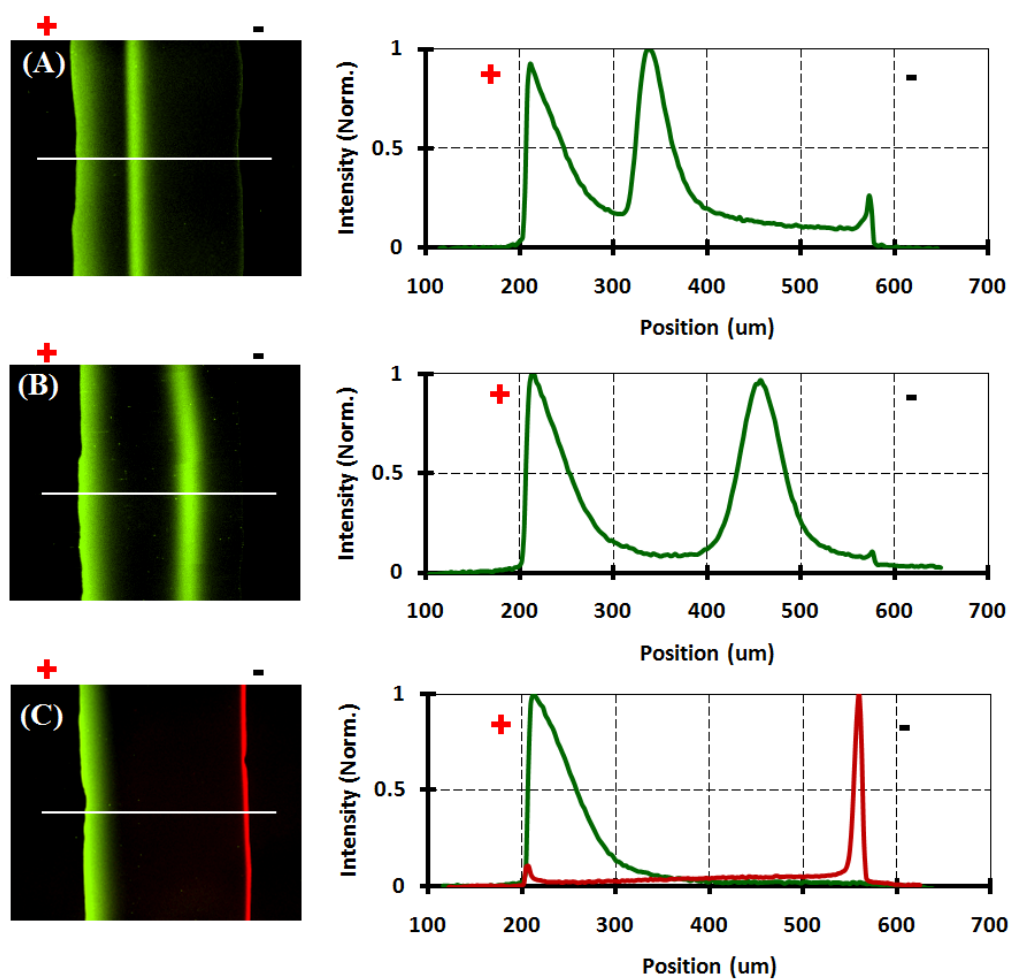


**Figure 9.** Electrophoretic-Electroosmotic Focusing of Individual Components. NBD-DPPE lipids were separated with different membrane-bound proteins, StrA-4 (A), StrA-1 (B) and IgG anti biotin (C) from homogeneous mixture in negatively charged lipid bilayer (10% POPG) in 50V/cm electric field. pH was 7.3, controlled by 10mM Tris buffer. The corresponding line-scan profile is on the right of each image.

As noted above, at steady state in an EEF experiment, there is a high POPG concentration near the anodic (left) edge of the SLB. This results in a high charge density at the anodic edge of the bilayer, and the charge density falls off to the right. Protein focusing takes advantage of this charge density gradient. The more negatively charged the protein, the closer it will focus to the positive electrode, due to the larger electrophoretic contribution. However, the larger the protein's cross section within the aqueous solution, the closer the focusing position will be to the negative electrode, due to the electroosmotic contribution. The steady state position of any protein results from the combination of these two counteracting forces. During the protein labeling process, Alexa-488 reacts with primary amine groups on the proteins, principally at lysine residues. As such, StrA-4 carries a larger negative charge than StrA-1 because the Alexa-488 dye molecules bear a net charge of -2 and replace the charge on the lysine, which was originally +1. Thus, for each labeled site, a net charge of -3 is added while the electroosmotic profile is nearly unchanged.<sup>29</sup> Thus, StrA-1 and the StrA-4 are separated from one another on the basis of differing charges. IgG has a molecular weight of about 150 kD, which is roughly three times greater than streptavidin. Therefore, the electroosmotic force on this protein is significantly larger and its motion is less dependent on its net charge. The estimated charge and radius of the proteins used in **Figure 8** are listed in the first two columns of **Table 1**.

**Table 1.** Charge, Radius and Zeta Potential of Proteins in the EEF Separation.

Estimated charge and radius of each component in the EEF separation were shown in **Figure 8**. The charge on a membrane-bound protein is the total charge on the labeled protein plus the charge on the bound biotin-cap-DOPE complex. Values for the charges and radii come from the associated references.

	Charge ( $e^-$ ) $Q_m^{43,44}$	Radius(nm) $r_m^{45,46}$	Zeta Potential (mV) $\zeta_m$
StrA 4	16	2.5	-62.8
StrA 1	7	2.5	-27.5
IgG	4	4.5	-6.39

## Discussion

The steady state position of a protein can be modeled mathematically by taking into account its electroosmotic profile and its charge. Specifically, a protein comes to rest at the position where  $\vec{F}_E + \vec{F}_{EO} = 0$ . The electrophoretic force on a membrane-bound protein<sup>20</sup> can be expressed by the following equation:

$$\vec{F}_E = 6\pi r_m \epsilon_r \epsilon_o \zeta_m \vec{E} \quad \text{Eq. 1}$$

$r_m$  is the radius of the protein,  $\epsilon_r$  is dielectric constant of aqueous phase and  $\epsilon_o$  is relative permittivity of free space,  $\zeta_m$  is the zeta potential of the protein and  $E$  is the external electric field .

Stokes dragging force (caused by electroosmotic flow) on a membrane-bound protein<sup>20</sup> can be expressed by the following equation:

$$\vec{F}_{EO} = 6\pi\eta_w r_m \vec{v}_{EO} \quad \text{Eq. 2}$$

$\eta_w$  is the viscosity of the solution,  $r_m$  is the radius of protein and  $v_{EO}$  is the electro-osmosis flow rate.  $v_{EO}$  is determined by **Eq. 3**,

$$\vec{v}_{EO} = -\frac{\vec{E} \epsilon_r \epsilon_o \zeta_{EO}}{\eta_w} \quad \text{Eq. 3}$$

$\zeta_{EO}$  is the zeta potential on surface,  $\epsilon_r$  is relative permittivity of the liquid and  $\epsilon_o$  is dielectric constant of vacuum. Putting **Eq. 3** into **Eq. 2**

$$\vec{F}_{EO} = -6\pi r_m \epsilon_r \epsilon_o \zeta_{EO} \vec{E} \quad \text{Eq. 4}$$

The dragging force on biotinylated lipid by the hydrophobic core of the lipid bilayer was always considered in previous studies. However, all components stop moving in our EEF experiment, the drifting velocity becomes zero. Therefore this dragging force becomes zero automatically.

At steady state,  $\vec{F}_E + \vec{F}_{EO} = 0$ , **Eq. 1** is equal to **Eq. 4**

$$\zeta_m = \zeta_{EO} \quad \text{Eq. 5}$$

where  $\zeta_{EO}$  is the zeta potential of the SLB (planar surface with thin diffusive double layer), while  $\zeta_m$  describes the zeta potential of a membrane-bound protein. Theoretically, the focusing takes place at the iso-zeta potential position, where the zeta potential of the protein is equal to the local zeta potential on the SLB.

Using this expression, one can calculate the relationship between the charge density on the membrane surface at the focusing position and the physical properties of the protein. Specifically, the zeta potential is:<sup>47</sup>

$$\zeta_m = \frac{Q_m \kappa^{-1}}{4\pi\epsilon r_m (\kappa^{-1} + r_m)} \quad \text{Eq. 6}$$

where  $Q_m$  is the charge on the protein,  $r_m$  is the radius of the protein,  $\kappa^{-1}$  is the Debye length and  $\epsilon$  is the permittivity of the electrolyte medium ( $7.08 \times 10^{-10} \text{ Fm}^{-1}$ ). The Debye length  $\kappa^{-1}$  is calculated by equation:

$$\kappa^{-1} = \sqrt{\frac{\epsilon_r \epsilon_0 kT}{2e^2 I N_A}} \quad \text{Eq. 7}$$

$k$  is Boltzman constant,  $T$  is temperature,  $I$  is ionic strength and  $N_A$  is Avogadro's constant. At 298 K, the Debye length  $\kappa^{-1}$  is  $\sim 3$  nm in a 10 mM buffer. The calculated values of  $\zeta_m$  for each protein employed in **Figure 8** are listed in **Table 1**.

The position dependent zeta potential of the SLB surface is related to the surface charge density  $\sigma_x$  as:<sup>47</sup>

$$\zeta_{EO} = \frac{\kappa^{-1} \sigma_x}{\epsilon} \quad \text{Eq. 8}$$

Due to the POPG gradient, the charge density of the SLB,  $\sigma_l$ , is a function of the position,  $x$  along the bilayer. An additional contribution,  $\sigma_g$ , comes from the charge on the glass substrate and is constant over the SLB. The total surface charge density  $\sigma_x$  is simply the summation of  $\sigma_l$  and  $\sigma_g$ . Thus,  $\sigma_x$  is a function of the lateral position along the SLB as:<sup>8</sup>

$$\sigma_x = \left( \sigma_g + \frac{\sigma_0}{\exp(-v_d(x-r_f)/D)+1} \right) \quad \text{Eq. 9}$$

where  $\sigma_0$  is the initial charge density of the SLB in the absence of an applied field,  $v_d$  is the drift velocity of POPG in the electric field,  $x$  is the position in the SLB parallel to the electric field,  $r_f$  is a constant with units of length and is related to the boundary conditions having the value of the width of the patterned bilayer section (380  $\mu\text{m}$ ).  $D$  is the diffusion constant of POPG.

Based on **Eq. 8 & 9**, the zeta potential of the SLB,  $\zeta_{EO}$ , at steady state can be plotted as a function of position along the direction of the electric field  $x$  (**Figure 10, top, red curve**).  $\sigma_0$  is calculated to be  $-24.3 \text{ mC/m}^2$  (see Supporting Information), assuming the area of a lipid to be  $0.66 \text{ nm}^2$ .<sup>48</sup> Also,  $-6 \text{ mC/m}^2$  was used for  $\sigma_g$  and  $0.08 \mu\text{m/s}$  for  $v_d$  in a  $50 \text{ V/cm}$  electric field with  $D = 3.5 \mu\text{m}^2/\text{s}$ .<sup>36,39,49</sup> The focusing positions are determined by matching the zeta potential of the proteins calculated by **Eq. 6** with the zeta potential of the SLB determined by **Eq. 8 & 9**. Proteins focus at positions where  $\zeta_m = \zeta_{EO}$ . The calculated focusing position of each component is marked by a vertical dashed line in **Figure 10** and is in good agreement with the experimental data.

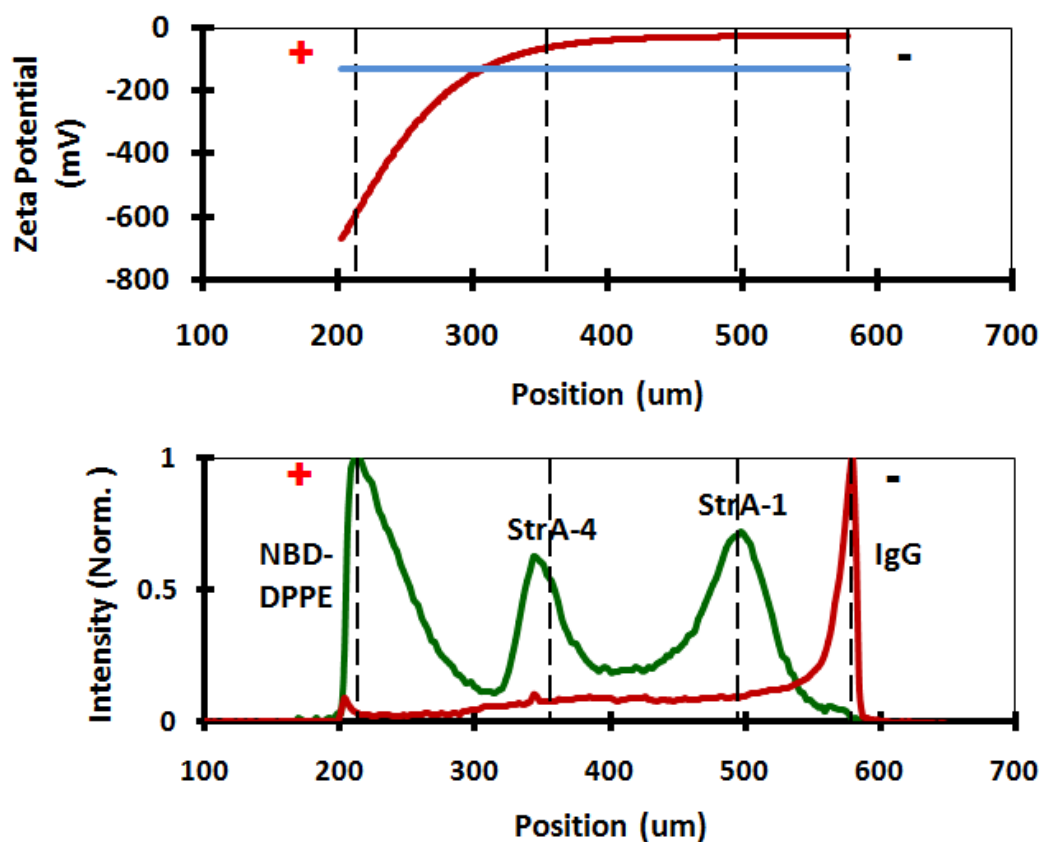


**Figure 10.** Calculation of Theoretical Focusing Positions. The top graph shows the zeta potential profile along a 10% POPG SLB before the application of an electric field (blue line) and at steady state after the application of a 50 V/cm field (red line). The dashed lines indicate the theoretical focusing positions of each component at steady state, as shown in **Table 1**. The bottom graph shows the fit of the calculated peak positions (vertical dashed lines) against the experimental line-scan profile after separation from **Figure 8**.

The initial migration direction of each charged membrane component can be predicted from the zeta potential before the POPG is redistributed (**Figure 10, top, blue line**). Moreover, the eventual focusing zeta potential values of the proteins (red curve) are at smaller zeta potential values than the initial value at uniform 10% POPG distribution. As such, the initial migration of all proteins was dominated by their respective electroosmotic forces. The value of the surface zeta potential at the IgG focusing position was smaller than the value of the zeta potential contributed by the glass substrate (-25.8 mV). Thus, this protein band was pushed to the right edge of the lipid bilayer. On the other hand, StrA 4 and StrA 1 first migrated one direction and then the other. NBD-DPPE did not protrude sufficiently far above the bilayer, so the electrophoretic force dominated the motion of the dye-labeled lipid under all conditions.

Combining **Eq. 8 & 9** reveals the relationship between the properties of each protein and its focusing position:

$$\sigma_x = \frac{Q_m}{4\pi\epsilon r_m(\kappa^{-1} + r_m)} \quad \text{Eq. 10}$$

As **Eq. 10** indicates, the focusing position of a protein depends on the Debye length, which is related to the ionic strength of the buffer. Physically, this translates into a major change in the electroosmotic force. A protein's focusing position also depends on the charge on the protein, which can be varied by changing the solution pH. **Eq. 9** also indicates that the POPG gradient is affected by the drift velocity of this lipid as determined by the electric field strength. By modulating these factors, the focusing positions of protein bands can be shifted quite substantially (**Figure 11, 12**). Careful tuning of the separation conditions may allow the separation of complex mixtures of



membrane proteins with only subtle differences. Because both electrophoretic force and electroosmotic force were affected by the Debye length to different extent, the change of ionic strength should change the focusing positions of the proteins. Based on **Eq. 10**, the increase of ionic strength should give a decrease of Debye length, so that the focusing positions of proteins should move to higher surface charge density regions. In **Figure 11**, the focusing positions of StrA-4 and StrA-1 were monitored under 1 mM, 10 mM and 25 mM pH 7.3 Tris buffer. In 10 mM Tris buffer, StrA-4 and StrA-1 were separated and focused at different positions on SLB. In 1 mM Tris buffer, both StrA-1 and StrA-4 were moved closer to the negative electrode side of the SLB, while they were all moved closer to the positive electrode side of the SLB in 25 mM Tris buffer. The influence of surface charge density gradient, which was determined by the percentage of negatively charged lipids and the electric field, was also observed in SLB containing 20% negatively charged POPG lipids (**Figure 12**). In 50 V/cm electric field, the surface charge gradient was broader. Therefore StrA-1 and StrA-4 were all focused near the negative electrode side of the SLB. When the electric field was increased to 100 V/cm, the surface charge gradient became narrower, so StrA-4 was able to move to a different position closer to the positive electrode side of the SLB.

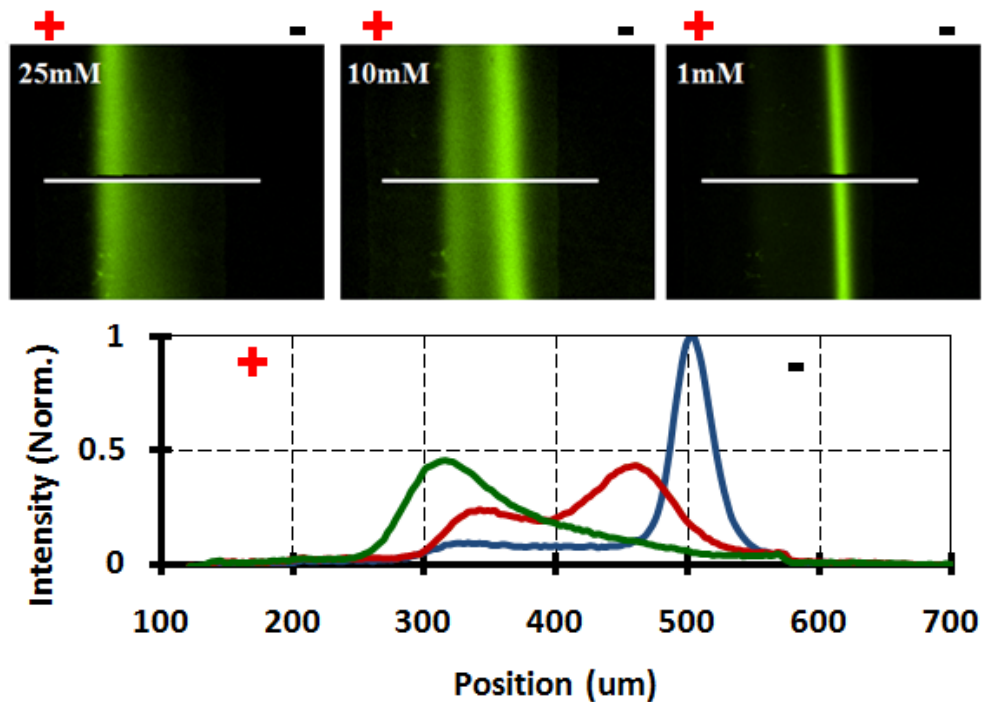


**Figure 11.** Effect of Buffer Ionic Strength. The migrations of StrA-4 and StrA-1 bands are monitored under three buffer concentrations on 10% POPG SLB, in 50 V/cm electric field. pH was 7.3, and ionic strengths were 25 mM, 10 mM and 1mM. The fluorescence pictures are on the top. The line-scan profiles of 25 mM (Green), 10 mM (Red) and 1 mM (Blue) buffer concentration are shown on the bottom. Based on **Eq. 10**, the increase of ionic strength (decrease of Debye length) should move all peaks to more negatively charged regions on SLB.

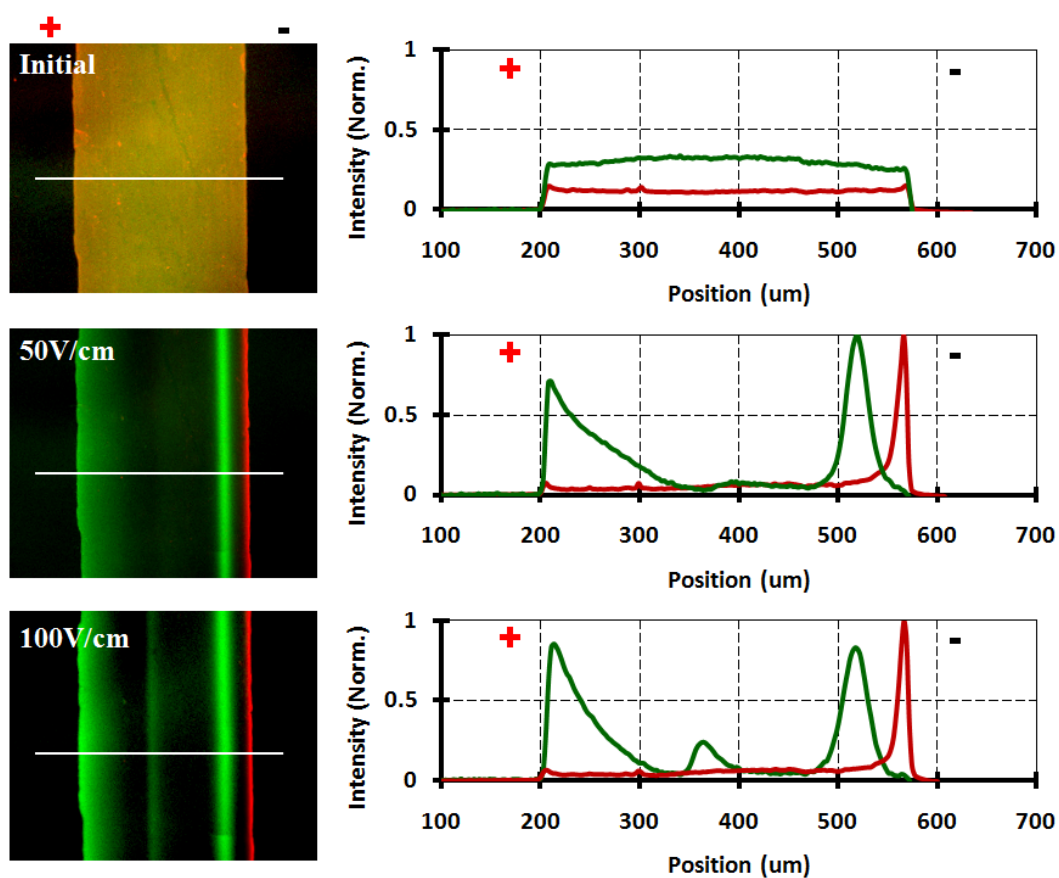


**Figure 12.** Effect of Negative Charge Density Gradient. The separation of protein and lipid mixture was done on 20% POPG SLB. Separation conditions were: 10 mM, pH 7.3 Tris buffer, both 50 V/cm and 100 V/cm electric field were used. Fluorescent images are on the left and the corresponding line-scan profiles are on the right. The bands on the bottom image from left to right are NBD-DPPE, StrA-4, StrA-1 and IgG. At 100 V/cm voltage, the negative charge gradient was more compressed than at 50V/cm, so that StreptAvidin peaks moved to the left, and two components were separated.

## Conclusions

EEF is ideally suited for work with trace membrane concentrations such as membrane proteins. This is because a large SLB area can provide for significant enrichment at the focusing location. Positively charged proteins could be separated in a similar manner as negatively charged species. In this case, the addition of positively charged lipids in an SLB would provide a positive charge gradient in an applied electric field. With sufficient positively charged lipid, the direction of electroosmotic flow could be switched, generating opposite electrophoretic and electroosmotic forces. In conclusion, we have demonstrated a new bilayer separation technique, EEF. This method can be used to separate, accumulate and potentially identify many components in protein-lipid mixtures on charged supported lipid bilayers. In the future, the separation and focusing of transmembrane proteins perhaps from native cell membranes could be accomplished with polymer or protein cushioned SLBs.<sup>6,50,51</sup>

CHAPTER III  
LABEL-FREE DETECTION OF COMPETITIVE BINDING  
ON SUPPORTED LIPID BILAYER

**Introduction**

Competitive bindings widely exist in cells and are involved in many important cellular processes, such as secretion, proliferation, differentiation, apoptosis, migration and protein transportation/insertion.<sup>52-59</sup> In the past decade, various label-free techniques have been developed based on ligand-receptor binding, but the detection of competitive binding is still challenging.<sup>56,60-69</sup> For example, the detection of biomarkers in serum requires the capability of simultaneous detection of multiple low concentration disease biomarkers in a background of a high abundance of proteins and interfering compounds.<sup>56,64</sup> Previously developed label-free detection techniques made use of the secondary effects caused by protein binding, such as surface plasmon resonance (SPR), surface acoustic wave (SAW), electrical signals from functionalized electrodes and nanowires, nanoparticle-based bio-barcode, microcantilever, optical microcavity resonator, nano-calorimeter, interferometer, and environmental sensitive fluorophores.<sup>56,60-69</sup> The signals generated by interfering molecules or nonspecific adsorptions cannot be discerned, because the origins of signals cannot be identified solely by the methods mentioned above. As a consequence, simultaneous detection of multiple proteins that bind to the same ligand cannot be achieved by these techniques.

To realize simultaneous label-free detection of multiple proteins that bind to the same ligand, we developed a novel separation-based label-free detection method on SLB by monitoring the steady-state focusing position of fluorescently labeled ligands based on the previously developed electrophoretic-electroosmotic focusing (EEF) technique.<sup>14</sup> In the EEF technique, proteins bound on the same kind of ligand can be separated and concentrated at different positions on SLB based on their size and charge ratio. Here, a fluorescently labeled ligand is added into the SLB and its EEF behavior in DC electric field is monitored. As illustrated in **Figure 13**, after the binding of proteins, the fluorescently labeled ligand in the SLB must experience a change of both electrophoretic force and electroosmotic force. This caused the focusing position of fluorescently labeled ligands to change dramatically upon protein binding. For different proteins, the changes of electrophoretic force and electroosmotic force on fluorescently labeled ligands are different. Therefore, the fluorescently labeled ligands bound with the same kind of protein will be focused to the same position. Since different proteins should be focused to different positions, multiple proteins that bind with the same ligand can be detected simultaneously. By monitoring the focusing behavior of fluorescently labeled ligands in SLBs, several unique properties and advantages could be obtained. First, only specific interactions can be detected. Non-specific adsorptions or interactions cannot generate any change to the movement of fluorescently labeled ligands, so the signal from non-specific interactions can be eliminated completely. Second, if each ligand contains the same number of fluorophores, the fluorescent intensity can directly reflect the amount of ligands. The fluorescent intensity ratio between protein-bound and free

ligands is directly related to the binding constant of the protein. Also, when the ratio of fluorescent intensities is taken, intensities of all components are automatically normalized, so that photo-bleaching effect can be eliminated. In the following experiments, we demonstrate the ability of detecting competitive binding of Streptavidin and IgG anti biotin on biotin-cap-NBDPE lipids (**Figure 13**).

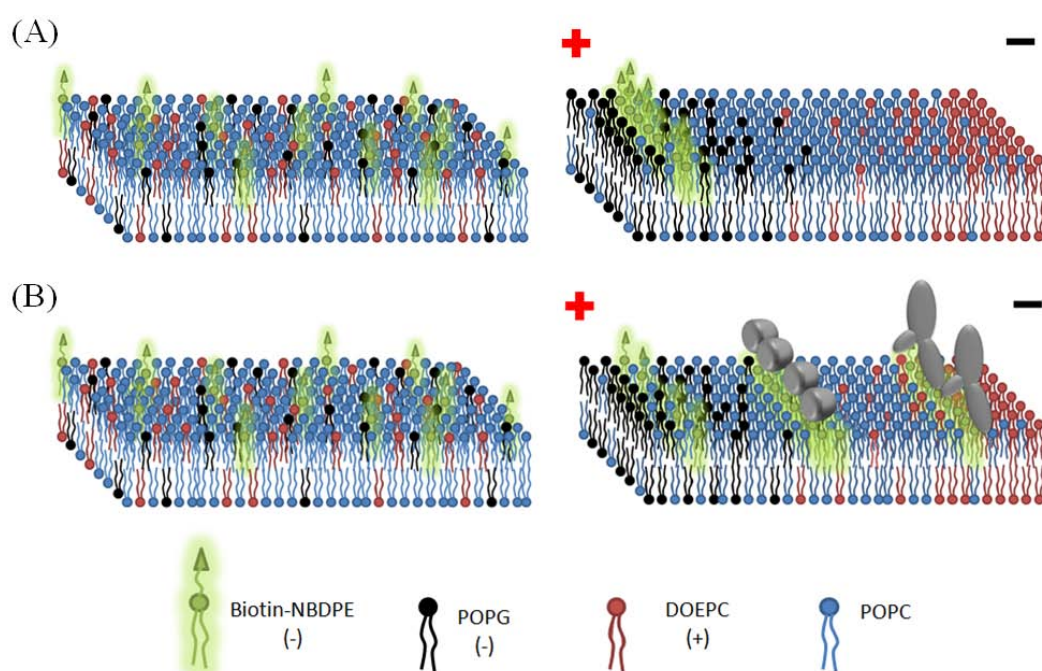


**Figure 13.** Illustration of Label-Free Detection of Protein Competitive Binding.

Fluorescent biotinylated lipid biotin-cap-NBDPE (represented by green color) is used as an indicator. (A) With no bound proteins, biotin-cap-NBDPE formed one band near to the positive electrode. (B) With the binding of proteins, several separated biotin-cap-NBDPE bands should be formed. Some biotin-cap-NBDPE lipids accumulated at different positions.

## Experimental Section

### Material

Fibrinogen and streptavidin were purchased from Sigma (St. Louis, MO). Goat anti biotin was purchased from Rockland Immunochemicals, Inc (Gilbertsville, PA). 1-palmitoyl-2-oleoyl-*sn*-glycero-3-phosphocholine (POPC), 1,2-dioleoyl-*sn*-glycero-3-ethylphosphocholine (DOEPC), 1-palmitoyl-2-oleoyl-*sn*-glycero-3-phospho-(1'-rac-glycerol) (POPG), 1,2-dipalmitoyl-*sn*-glycero-3-phosphoethanolamine-*N*-(7-nitro-2-1,3-benzoxadiazol-4-yl) (NBDPE), and 1,2-dioleoyl-*sn*-glycero-3-phosphoethanolamine-*N*-[methoxy(polyethylene glycol)-550] (PEG550-DOPE) were purchased from Avanti Polar Lipids (Alabaster, AL). NHS-LC-Biotin was purchased from ProteoChem (Denver, CO). Polydimethylsiloxane (PDMS) was obtained from Dow Corning (Sylgard, silicone elastomer-184).

### Synthesis of Biotinylated NBDPE (Biotin-cap-NBDPE)

1 mg of 18:1-12:0 NBDPE and 0.62 mg succinimidyl 6-(biotinamido) Hexanoate (NHS-LC-Biotin) were dissolved and mixed in 200  $\mu$ l anhydrous dichloromethane. Then 0.15  $\mu$ l triethylamine was added to the solution and the mixture was stirred at room temperature for 48 hours. The reaction was shown in **Figure 14**. NHS-LC-Biotin and 18:1-12:0 NBDPE were linked together through –CO-NH- peptide bond. The products were separated and purified by Silica Gel TLC plate with mixed solvent ( $\text{CH}_2\text{Cl}_2$  and



Methanol 9:1). MS spectrum of the purified sample was also taken, and used to verify the formation of the target molecule (**Figure 14**).

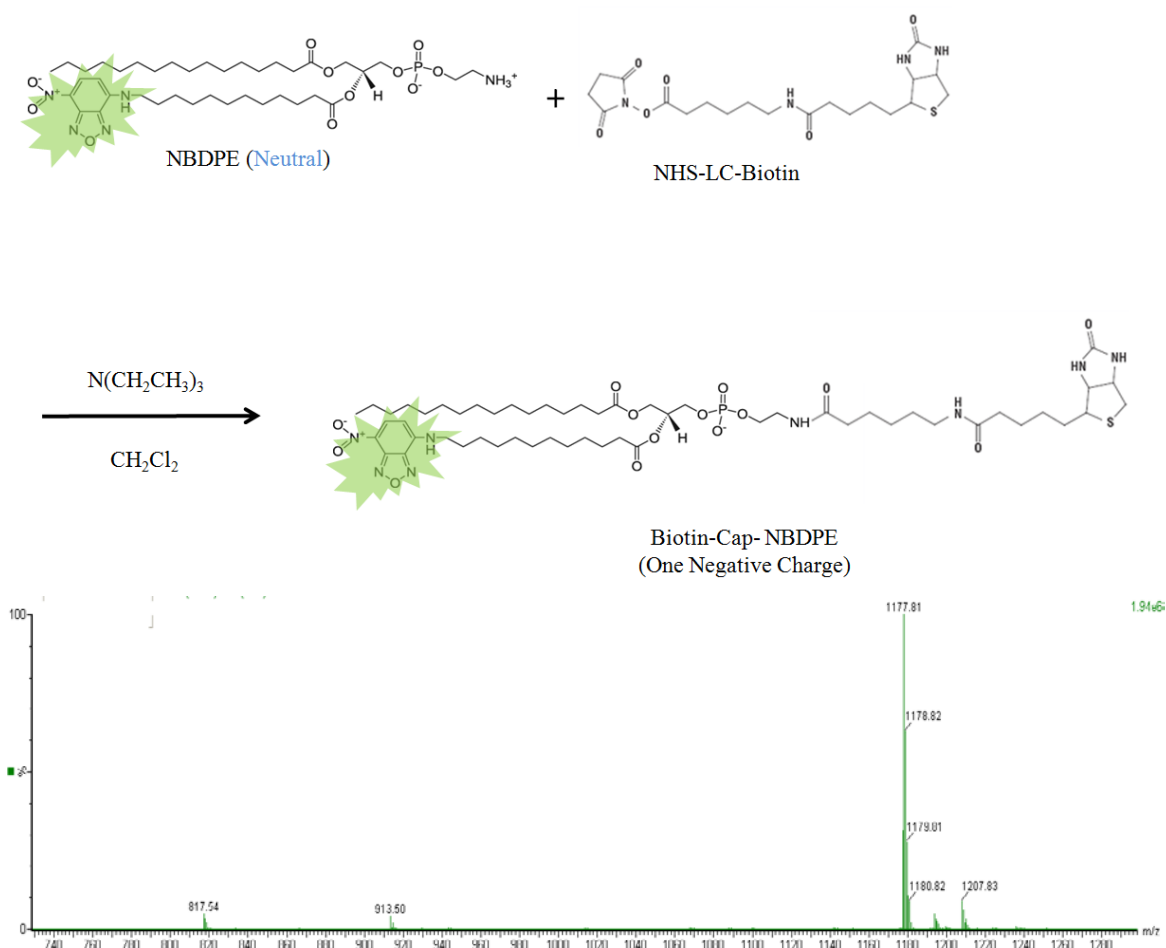


**Figure 14.** Synthesis of Biotin-cap-NBDPE. The synthesis procedure and ESI MS spectrum of the purified product. The molecular weight of biotin-cap-NBDPE is 1177.81.

## PDMS Stamp and SLB Patterning

PDMS monomer and cross-linker were mixed in a 10:1 mass ratio. The mixture was stirred and vacuum degassed. PDMS was then poured over a patterned glass mold and cured at room temperature overnight. The glass master consisted of a series of ten 380  $\mu\text{m}$  wide parallel lines that were 1 cm long and separated from one another by 200  $\mu\text{m}$  spacers. The glass master was prepared using standard HF etching techniques described previously.<sup>4</sup> The PDMS stamp was carefully peeled away from the glass, washed with ethanol, and rinsed with purified water. In all experiments performed herein, each SLB patch was about 380  $\mu\text{m}$  wide and isolated from the adjacent region by a fibrinogen monolayer adsorbed onto the planar glass substrate. To form SLB patches, a PDMS stamp was placed on a clean cover glass slide. A 1.0 mg/mL fibrinogen solution (in 10mM PBS buffer) was added to form a fibrinogen monolayer on the exposed glass area. After 1 hour incubation, the fibrinogen was rinsed away with 10 mM Tris buffer, and the PDMS stamp was removed. Finally, a 1 mg/mL lipid vesicle solution was introduced and SLBs formed spontaneously on the area without the fibrinogen monolayer.<sup>70</sup>

## SLB Formation

SLBs were formed by the vesicle fusion method<sup>7,21</sup> on clean glass coverslips (Corning, NY, 22 $\times$ 22 mm, No. 2). The coverslips were cleaned in a boiling 1:3 solution of 7X detergent (MP Biomedicals, Solon, OH) and purified water. Purified water came from an Ultrapure Water System (Thermo Scientific Barnstead Nanopure Life Science,

Marietta, OH). The coverslips were rinsed with copious amounts of purified water, dried with nitrogen, and annealed in a kiln at 500 °C for 5 h before use. Small unilamellar vesicles (SUVs) with 10% DOEPC, 3% POPG, 1% PEG550-DOPE, 0.25% biotin-cap-NBDPE and 85.75% POPC were prepared by vesicle extrusion. To do this, the lipids were mixed in chloroform. The chloroform was subsequently evaporated under a stream of nitrogen followed by vacuum desiccation for 4 h. Then the lipids were rehydrated in phosphate buffered saline (PBS) solution which consisted of 10 mM sodium phosphate, 150 mM NaCl, and 0.2 mM sodium azide. The pH of the PBS solution was tuned to 7.4 with a small amount of 1M HCl. The concentration of the lipids in solution was 1.0 mg/mL. After several freeze-thaw cycles, the solutions were extruded through a polycarbonate filter (Whatman) with 100 nm pores.

#### Introduction of Target Proteins

Goat anti biotin and Streptavidin were diluted from 1 mg/mL stock solution by 1 mg/mL BSA solution in 10mM Tris and 100mM NaCl buffer. 200 $\mu$ L diluted protein solution was added to the patterned SLB and incubated for long enough time (usually 2 hours) to reach the equilibrium. In order to keep the bulk concentration constant and eliminating the depletion effect near the SLB surface during the incubation process, the solution was stirred constantly by pipetting. After incubation, the bulk protein solution was rinsed off by 10mM Tris and 100mM NaCl buffer. Then the sample was incorporated into the flow cell device.

## Fluorescence Imaging and Flow Cell

Epifluorescence images were obtained using a Nikon E800 fluorescence microscope with a Roper Scientific MicroMAX 1024B charge-coupled device (CCD) camera (Princeton Instruments). The experimental conditions during EEF experiments were well controlled by using a flow cell device,<sup>29</sup> with pH 8.0 10mM Tris and 100 mM NaCl buffer. 75 V/cm electric potential was applied across the bilayers. The buffer flow rate of each channel was 120 mL/hour.

## Results

### Migration of Biotin-cap-NBDPE in SLB

Under near neutral pH, the biotinylation of zwitterionic NBDPE lipids eliminated a positive charge on the primary amine of NBDPE head group. Therefore the product, biotin-cap-NBDPE has one negative charge. We monitored the migration of 0.1% biotin-cap-NBDPE lipids in 3% POPG, 1% PEG550-DOPE, 10% DOEPC and 95.9% POPC lipid bilayer. 10mM pH 8.0 Tris with 100mM NaCl buffer was used to control the pH inside the flow cell device. As illustrated in **Figure 15**, the fluorescent biotin-cap-NBDPE lipids were evenly distributed in the whole lipid bilayer patch. After the application of 50V/cm electric field parallel to the bilayer for about 30 minutes, the biotin-cap-NBDPE lipids were focused near to the positive electrode side of the SLB patch. Negatively charged POPG piled up against the positive electrode side of the SLB and formed a negative charge density gradient in the SLB. Meanwhile, positively

charged DOEPC piled up against the negative electrode side of the SLB. Due to the electroosmotic effect<sup>14</sup> and lipid de-mixing effect<sup>8</sup> generated by negatively charged POPG lipids, biotin-cap-NBDPE lipids were not directly piled up against the boundary of the lipid bilayer patch. The formation of a single Gaussian peak by biotin-cap-NBDPE also proved the purity of the synthesized biotin-cap-NBDPE lipids.

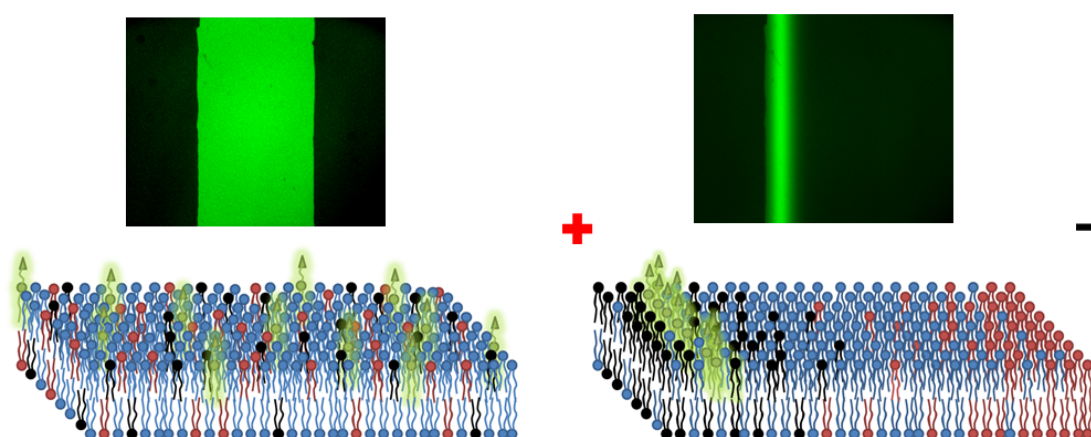


**Figure 15.** Focusing of Biotin-cap-NBDPE Lipids. Biotin-cap-NBDPE lipids were focused in charged lipid bilayer, in 50V/cm electric field. pH was 8, controlled by 10mM Tris buffer with 100mM NaCl. The charged lipid bilayer contained 0.1% biotin-cap-NBDPE, 10% POEPC, 3% POPG, 1% PEG550-DOPE and 85.9% POPC.

#### Label-Free Detection of Goat Anti Biotin

Herein, we used two different proteins that bind to the same biotin ligand on SLBs. The first protein tested was goat anti biotin. goat anti biotin has a pI of 7- 8.<sup>71</sup> Under the experimental conditions (10mM pH 8.0 Tris with 100mM NaCl buffer), the protein was nearly uncharged. Therefore the charge of the protein-lipid complex was not

changed obviously upon goat anti biotin binding. On the other hand, the radius of goat anti biotin above the SLB was about  $4.5 \text{ nm}^{45}$ , so the electroosmotic force on the protein-lipid complex should be dramatically increased compared to biotin-cap-NBDPE lipids. Based on the focusing theory, this protein-lipid complex should get focused at a lower negative charge density position than the biotin-cap-NBDPE lipids. Besides the biotin-cap-NBDPE lipids bound with goat anti biotin, there should be also free biotin-cap-NBDPE lipids in the SLB not bound to goat anti biotin. Thus, the biotin-cap-NBDPE lipids should finally be divided into two populations, which would be separated and focused at two different positions in the SLB.

Goat anti biotin in 1mg/mL BSA, 10mM Tris and 100mM NaCl solution was used in the following experiments. The EEF experiments were performed in 10mM pH 8.0 Tris with 100mM NaCl buffer. As illustrated in **Figure 16**, the focusing experiment was performed by incubating the SLB with 333 pM goat anti biotin, and the fluorescent biotin-cap-NBDPE lipids were focused and separated into two distinct peaks. The peak near to the positive electrode side of the SLB was formed by free biotin-cap-NBDPE lipids. The other peak near to the negative electrode side of the SLB was formed by goat anti biotin bound biotin-cap-NBDPE, because the addition of goat anti biotin on biotin-cap-NBDPE gave a huge increase of electroosmotic force on the protein-lipids complex. Positively charged DOEPC lipids also accumulated near the negative electrode side of the bilayer, so that the goat anti biotin bound biotin-cap-NBDPE peak was pushed off the edge of the SLB.

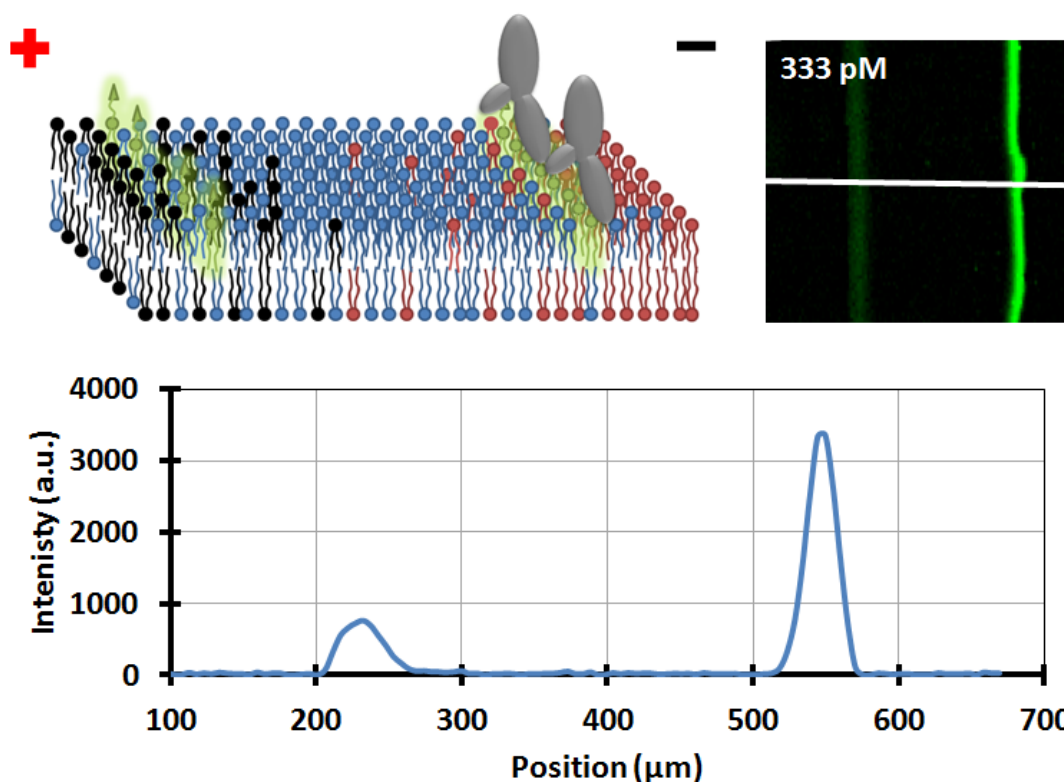


**Figure 16.** Label-Free Detection of Goat Anti Biotin. The experiment was done in 50 V/cm electric field. pH was 8, controlled by 10mM Tris buffer with 100mM NaCl. The corresponding line-scan profile is on the right of the image. Biotin-cap-NBDPE lipids are separated into two peaks upon goat anti biotin binding. The peak near to the positive electrode side of the SLB patch is free biotin-cap-NBDPE lipids, and the other peak near the negative electrode side of the SLB patch is goat anti biotin bound biotin-cap-NBDPE lipids.

The fraction of goat anti biotin bound biotin-cap-NBDPE lipids directly reflects the amount of goat anti biotin bound on surface, since each goat anti biotin binds with two biotin-cap-NBDPE lipids before the saturation point. Therefore, a unique advantage

of this system is that the percentage of both free ligands and protein bound ligands can be read out directly. By integrating the fluorescent intensities of each peak, it is easy to calculate the fraction of biotin-cap-NBDPE lipids that were bound to goat anti biotin. The saturation curve of goat anti biotin was generated by incubating the SLB with different concentrations of goat anti biotin (**Figure 17**). The limit of detection of goat anti biotin was determined to be about 6 pM (**Figure 18**). In fact, the fluorescent intensities of all peaks were normalized, which eliminated the fluorescence quenching effect by the light source. Moreover, the nonspecific adsorption of proteins on SLBs was not detected, because the nonspecific adsorptions cannot affect the focusing position of biotin-cap-NBDPE lipids.

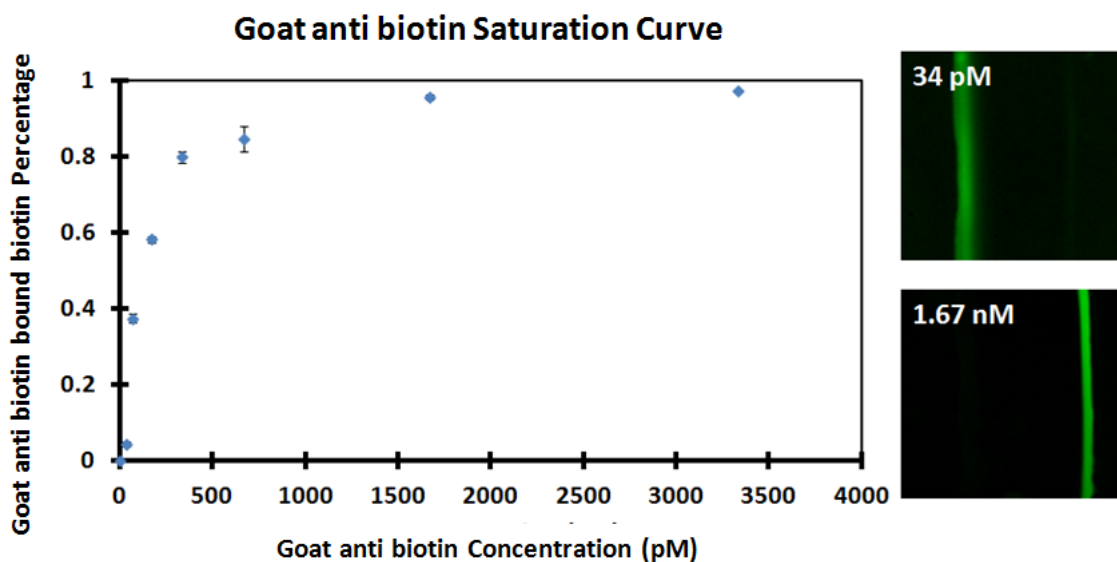


**Figure 17.** Saturation Curve of Goat Anti Biotin. The fluorescent intensity of the entire SLB patch was normalized, and the percentage of the total fluorescent intensity of goat anti biotin bound biotin-cap-NBDPE was calculated.



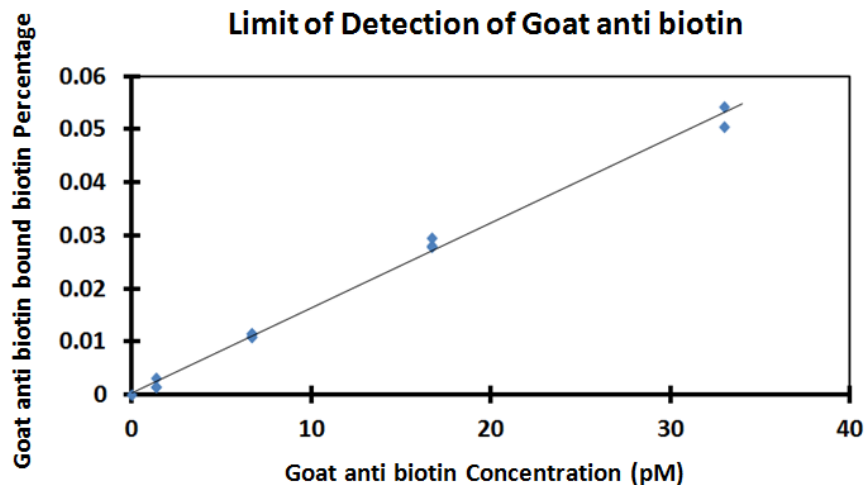


**Figure 18.** Limit of Detection of Goat Anti Biotin. The fluorescent intensity of the entire SLB patch was normalized, and the percentage of the total fluorescent intensity of goat anti biotin bound biotin-cap-NBDPE was calculated.

#### Label-Free Detection of Streptavidin

Streptavidin has a pI of about 5.<sup>44</sup> Under the same experimental conditions as mentioned above, each Streptavidin has two negative charges. The radius of Streptavidin is about 2.5 nm,<sup>46</sup> which is much smaller than goat anti biotin. According to the EEF focusing theory, Streptavidin bound biotin-cap-NBDPE lipids should get focused at a higher negative charge density position compared to goat anti biotin bound biotin-cap-NBDPE lipids. In **Figure 19**, the focusing experiment was performed with SLB incubated with 83 pM Streptavidin, and the fluorescent biotin-cap-NBDPE lipids were again focused and separated into two distinct peaks. Compared to goat anti biotin bound biotin-cap-NBDPE, Streptavidin bound biotin-cap-NBDPE lipids were focused closer to the positive electrode side of the SLB, where the negative charge density was higher.

The saturation curve of Streptavidin was generated by incubating the SLB with several Streptavidin concentrations (**Figure 20**). The limit of detection of Streptavidin was determined to be 600 fM. From the saturation curves of goat anti biotin and Streptavidin, it is clear that Streptavidin has higher binding affinity to biotin-cap-NBDPE than goat anti biotin on SLB.

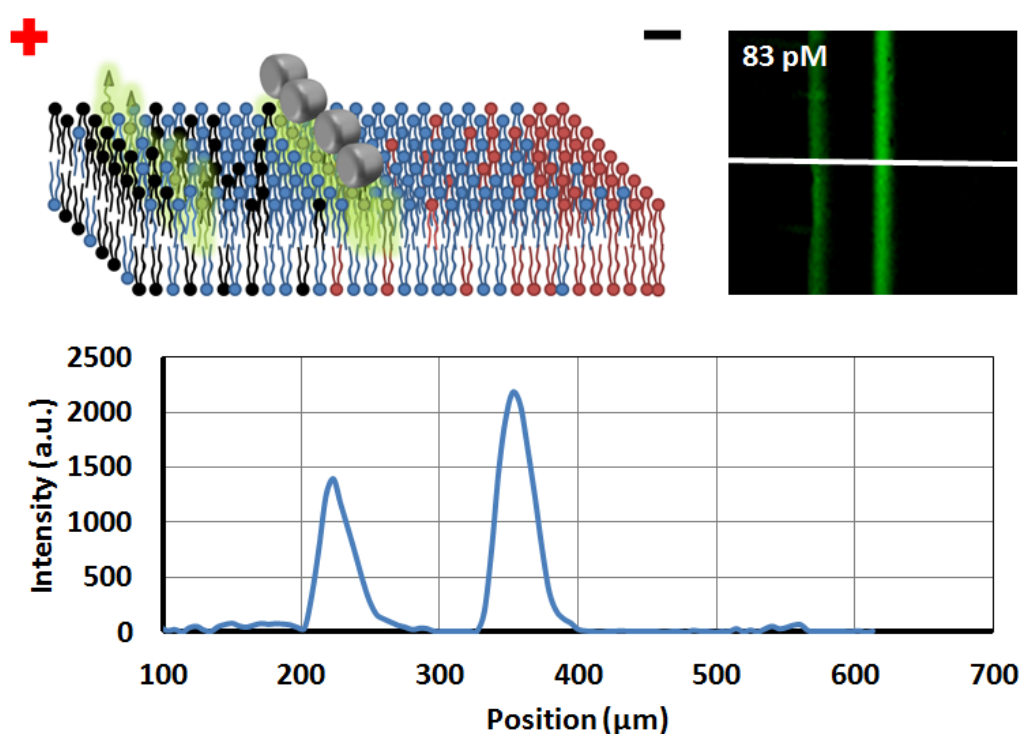


**Figure 19.** Label-Free Detection of Streptavidin. The experiment was done in 50 V/cm electric field. The pH was 8, controlled by 10mM Tris buffer with 100mM NaCl. The corresponding line-scan profile is on the bottom. Biotin-cap-NBDPE lipids were separated into two peaks upon Streptavidin binding. The peak near to the positive electrode side of the SLB patch is free biotin-cap-NBDPE lipids, and the other peak in the middle of the SLB patch is Streptavidin bound biotin-cap-NBDPE lipids.

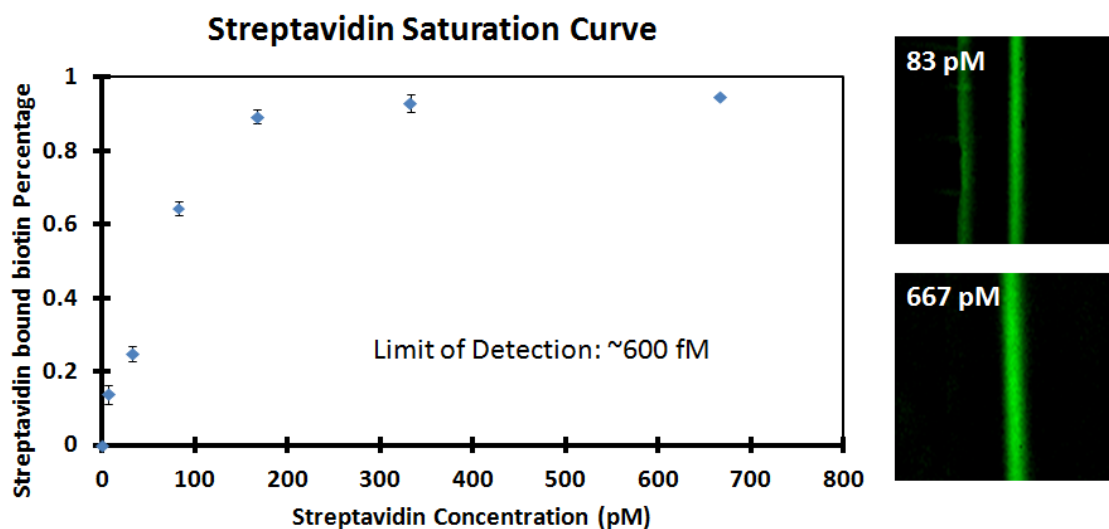


**Figure 20.** Saturation Curve of Streptavidin. The fluorescent intensity of the entire SLB patch was normalized, and the percentage of the total fluorescent intensity of Streptavidin bound biotin-cap-NBDPE was calculated.

#### Simultaneous Detection of Multiple Proteins and Competitive Binding

As illustrated above, we successfully detected goat anti biotin and Streptavidin using EEF focusing method. Particularly, the separation based label-free detection method enabled the detection of multiple proteins that bind to the same ligand on surface, which cannot be done easily by non-separation based label-free detection techniques. Here we detected goat anti biotin and Streptavidin mixture simultaneously in a single SLB patch.

The total concentration of goat anti biotin and Streptavidin was kept at 1 nM. Four different bulk protein concentration combinations were used, they were 167/833 pM, 333/667 pM, 667/333 pM and 833/167 pM (goat anti biotin/Streptavidin). All proteins were premixed in solution, and then incubated with SLBs. In **Figure 21**, biotin-cap-NBDPE lipids were focused and separated into three distinct peaks. By varying the concentrations of Streptavidin and goat anti biotin, the peaks can be easily identified. The peaks from left to right corresponded to free biotin-cap-NBDPE, Streptavidin bound biotin-cap-NBDPE and goat anti biotin bound biotin-cap-NBDPE. The focusing positions of Streptavidin bound biotin-cap-NBDPE and goat anti biotin bound biotin-cap-NBDPE were not affected by the addition of another protein, compared to the focusing positions in their individual experiments. Thus, we successfully detected multiple proteins that bind or interact with the same substrate by a separation based label-free method.

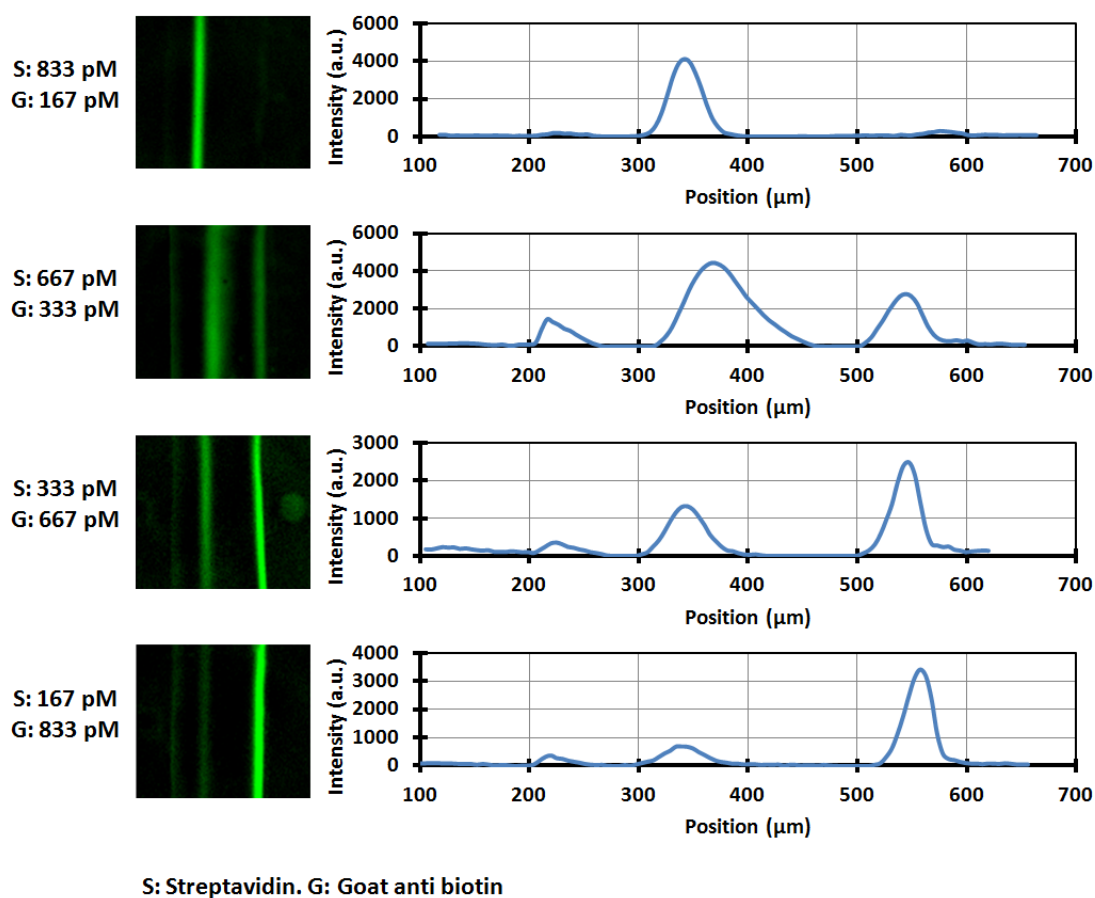


**Figure 21.** Simultaneous Detection of Streptavidin and Goat Anti Biotin. The experiments were done in 50 V/cm electric field. pH was 8, controlled by 10mM Tris buffer with 100mM NaCl. Two of the line-scan profiles are shown on the bottom. Biotin-cap-NBDPE lipids are separated into three peaks, from left to right, they are free biotin-cap-NBDPE lipids, Streptavidin bound biotin-cap-NBDPE lipids and goat anti biotin bound biotin-cap-NBDPE lipids.

Furthermore, the competitive binding of Streptavidin and goat anti biotin was studied. Once the bulk concentration of goat anti biotin (weaker binding) was held constant, the increase of Streptavidin (stronger binding) bulk concentration should decrease the amount goat anti biotin bound on SLB surface, simply because Streptavidin should compete for the same binding sites with goat anti biotin. Two series of experiments were conducted with 333 pM and 667 pM goat anti biotin in bulk respectively. In each series of experiments, the bulk concentration of goat anti biotin was kept constant, while the bulk concentration of Streptavidin was varied from 0 pM to 833 pM. All proteins were premixed in solution before incubating with the SLBs. The results were shown in **Figure 22**. The goat anti biotin bound biotin-cap-NBDPE fraction decreased obviously with the increase of bulk Streptavidin concentration. Finally, this decrease slowed down and then leveled off even if the Streptavidin bulk concentration got higher. No matter how high the stronger binding protein (Streptavidin) concentration was, there were always some binding sites that were occupied by the weaker binding protein. With 333 pM goat anti biotin bulk concentration, the fraction of goat anti biotin bound biotin-cap-NBDPE decreased from 80% to 20% as Streptavidin bulk concentration increased from 0 pM to 833 pM. At equal goat anti biotin and Streptavidin bulk concentration (333 pM), goat anti biotin and Streptavidin occupied 32% and 60% biotin-cap-NBDPE respectively, which indicated that Streptavidin bound tighter. With 667 pM goat anti biotin bulk concentration, the fraction of goat anti biotin bound biotin-cap-NBDPE decreased from 88% to 43% as Streptavidin bulk concentration increased from 0 pM to 833 pM. At equal goat anti biotin and Streptavidin bulk concentration (667

pM), goat anti biotin and Streptavidin occupied 45% and 49% biotin-cap-NBDPE respectively.

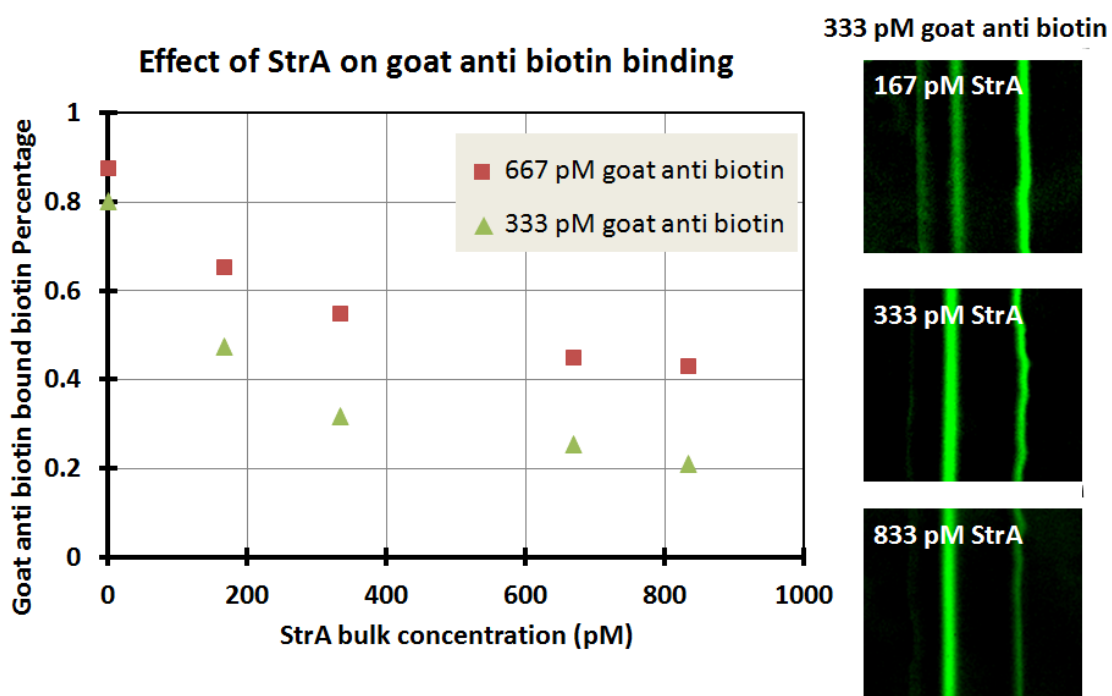


**Figure 22.** Label-Free Detection of Competitive Binding. Competitive binding between Streptavidin and goat anti biotin on biotin-cap-NBDPE were monitored in charged lipid bilayer. The amount of membrane-bound goat anti biotin decreased with the addition of Streptavidin, because they competed for the same binding sites on bilayer. The concentrations were the protein concentrations in bulk.

From the chart in **Figure 22**, There are several phenomenon caused by the competitive binding between goat anti biotin and Streptavidin. First, it is very interesting to note that the apparent binding affinity difference between goat anti biotin and Streptavidin is more significant at lower protein concentrations. And the decrease of goat anti biotin bound biotin-cap-NBDPE fraction caused by 833 pM Streptavidin was larger at 333 pM goat anti biotin (60%) than 667 pM (45%). Second, with 833 pM Streptavidin, the goat anti biotin bound biotin-cap-NBDPE fraction in 333 pM and 667 pM goat anti biotin were 20% and 43% respectively. Under high Streptavidin concentrations, the fraction of goat anti biotin bound biotin-cap-NBDPE had a almost linear relationship with goat anti biotin bulk concentration. Third, we plotted the Streptavidin/goat anti biotin ratio on surface versus the Streptavidin/goat anti biotin ratio in bulk (**Figure 23**). The slopes of the linear fitting in **Figure 23** were 1.4 in 333 pM goat anti biotin and 1.1 in 667 pM goat anti biotin. This result indicated that the stronger binding protein (Streptavidin) can inhibit the binding of weaker binding protein (goat anti biotin) more strongly at lower weaker binding protein concentrations.



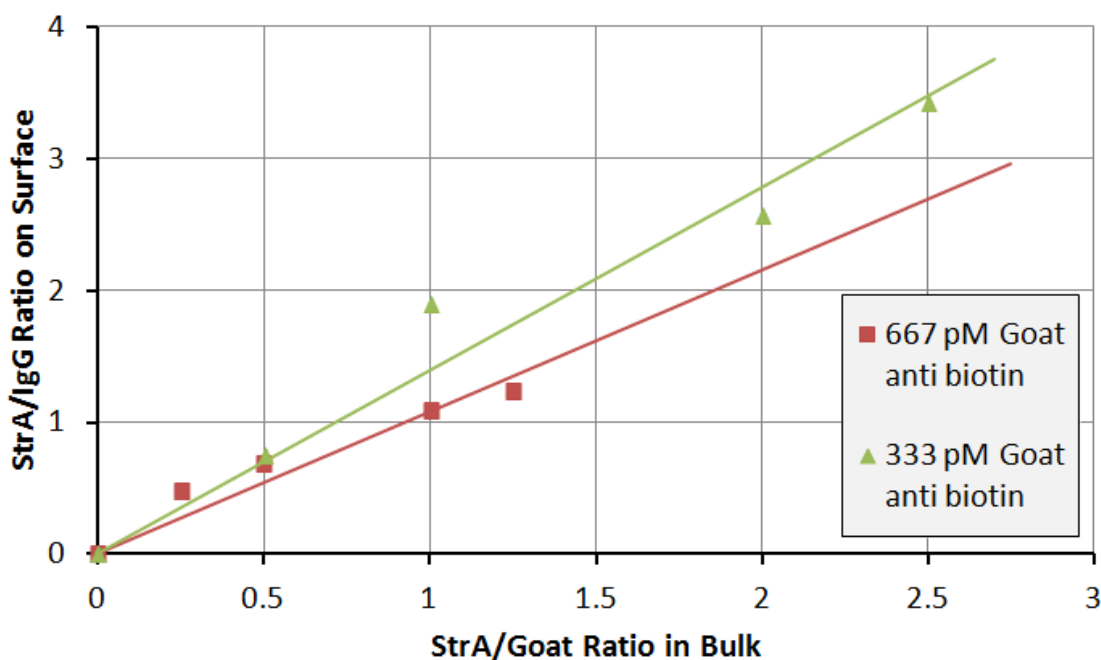


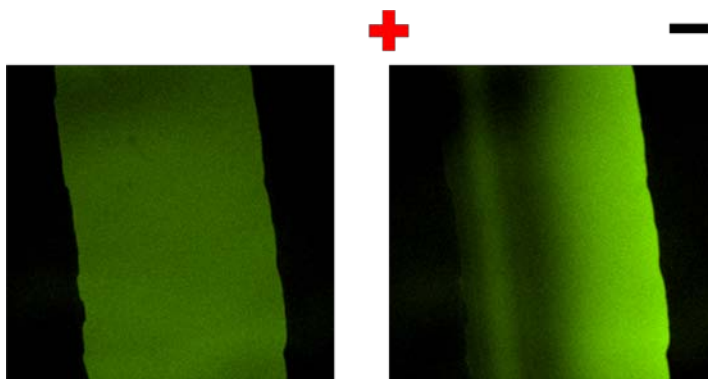
**Figure 23.** Inhibition of Goat Anti Biotin Binding by Streptavidin. The concentration ratio of Streptavidin and goat anti biotin bound on SLB was plotted against the concentration ratio of Streptavidin and goat anti biotin in bulk solution. It could be observed that the inhibition of goat anti biotin by Streptavidin was more severe when the goat anti biotin concentration was low. At high goat anti biotin concentration, Streptavidin and goat anti biotin showed similar apparent binding affinity.

## Discussion

### Selection of Separation Conditions

Based on theoretical calculations,<sup>14</sup> unlabeled Streptavidin should be pushed close to the edge of the negative electrode side of the SLB in 10 mM Tris pH 7.3 buffer, due to the strong electroosmotic force. In 10 mM Tris pH 7.3 buffer, Streptavidin was

moved to nearly the same position as goat anti biotin, which showed great consistency with the calculation (**Figure 24**). In order to resolve Streptavidin and goat anti biotin peaks, we increased the buffer pH to 8.0 and added 100 mM NaCl to increase the ionic strength. The measurements could increase protein negative charge and decrease electroosmotic force on proteins. In 10 mM Tris, 100 mM NaCl pH 8.0 buffer, Streptavidin band was moved to the middle of the SLB, while goat anti biotin band was kept almost at the same position. Goat anti biotin was still close to neutral at pH 8.0, so the migration was still dominated by electroosmotic force.

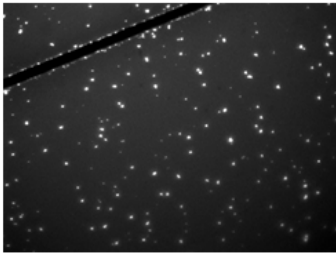
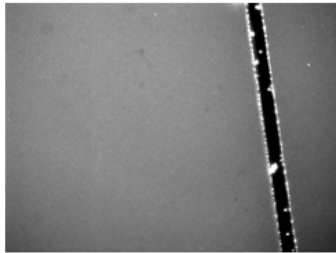
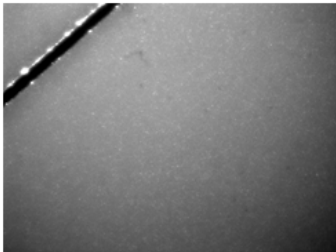
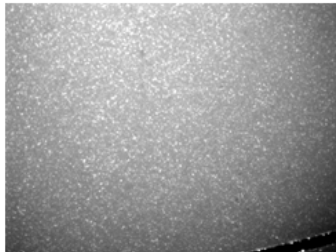


**Figure 24.** Detection of Streptavidin in Low Ionic Strength Condition. Streptavidin biotin-cap-NBDPE lipids were focused in 50 V/cm electric field. The pH was 8, controlled by 10mM Tris without extra salt. The charged lipid bilayer contained 0.1% biotin-cap-NBDPE, 10% POEPC, 3% POPG, 1% PEG550-DOPE and 85.9% POPC. Due to the stronger electroosmotic force on Streptavidin at low salt concentration, Streptavidin bound biotin-cap-NBDPE lipids were pushed to the negative electrode side of the SLB patch.

### Effect of Positively Charged DOEPC Lipids

DOEPC lipids were mixed in the SLBs in order to form positive charge density gradient and push membrane bound proteins off SLB edges. Another important reason was to generate a net positive charge on the SLBs, so as to prevent the clustering of Streptavidin molecules bound on SLB surface during incubation in high ionic strength buffer. On SLBs containing 10% negatively charged POPG lipids, biotin-cap-NBDPE lipids clusters were observed after the incubation of SLBs with Streptavidin in 10 mM Tris 100 mM NaCl buffer (**Figure 25**). However, no obvious biotin-cap-NBDPE lipids clusters were observed after the incubation of SLBs with Streptavidin in 10 mM Tris buffer or lower ionic strength buffer. Similar clustering behavior of fluorescently labeled Streptavidins was also observed on SLBs with POPG lipids and biotinylated lipids.<sup>14</sup> The degree of biotin-cap-NBDPE clustering was also found to be a function of Streptavidin concentration. Accordingly, the biotin-cap-NBDPE clustering behavior was assumed to be associated with the electrostatic interactions between the negatively charged membrane-bound Streptavidins and negatively charged lipids in SLBs. Based on this assumption, the addition of positively charged DOEPC lipids should disrupt this electrostatic interaction and eliminate biotin-cap-NBDPE clusters caused by Streptavidin binding in high ionic strength buffer. In **Figure 25**, it clearly showed that no biotin-cap-NBDPE lipids clusters were observed on SLBs containing 10 % positively charged DOEPC lipids in 10 mM Tris 100 mM NaCl buffer. Similarly, positively charged Avidin binding on positively charged SLB (10 % DOPEC) in 10 mM Tris 100 mM NaCl buffer also caused biotin-cap-NBDPE cluster formation (**Figure 25**). Biotin-cap-NBDPE

clusters caused by positively charged Avidin binding on positively charged SLBs were also eliminated by switching the net charge on SLB to negative (10 % POPG).

	<b>Negative Charged Protein:</b> Streptavidin, 30nM	<b>Positive Charged Protein</b> Avidin, 30nM
<b>Negative Charged Bilayer:</b> 10% POPG 89% POPC 1% Biotin-NBDPE		
<b>Positive Charged Bilayer:</b> 10% DOEPC 89% POPC 1% Biotin-NBDPE		

**Figure 25.** Effect of Surface Charge on Ligands Clustering. The clustering of membrane-bound protein was found to be related to the charges of both protein and SLB surface.

#### Detection Time Affected by SLB Width

The detection time should be shortened by using narrower SLBs. The EEF experiment was also done in 250  $\mu\text{m}$  wide SLBs. The three components were also well separated, and the relative focusing position was the same as in 400  $\mu\text{m}$  SLBs (**Figure 26**). Because the width of lipid bilayer was narrower, the time required for the migration

and accumulation of lipids and proteins became shorter than in 400  $\mu\text{m}$  wide SLBs. The final steady state was reached in 20 minutes. In literature, the smallest SLBs formed by vesicle fusion method was about 100 nm in width.<sup>26</sup> Thus, the detection time could potentially be reduced to seconds or sub-seconds scale.

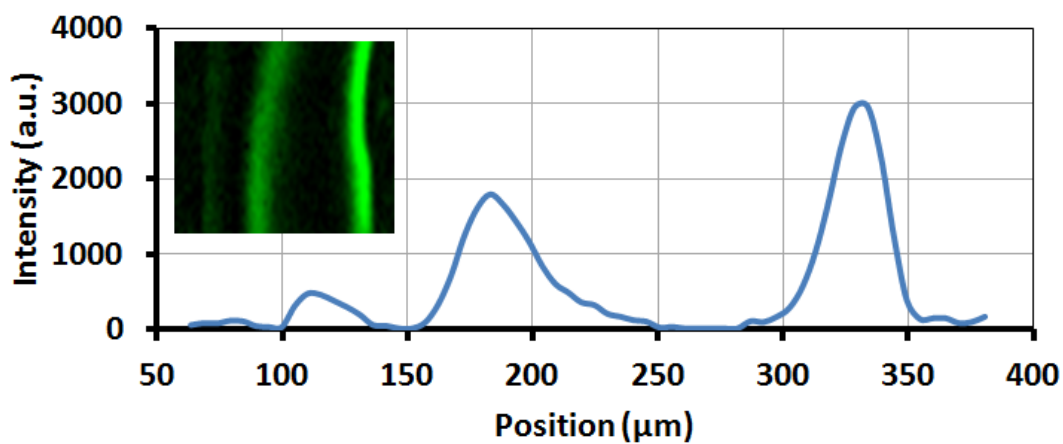


**Figure 26.** Detection in Narrower SLB. Streptavidin and goat anti biotin were detected simultaneously using biotin-cap-NBDPE in 250  $\mu\text{m}$  wide SLB, in 50V/cm electric field. pH was 8, controlled by 10mM Tris buffer with 100mM NaCl.

## Conclusions

In conclusion, we developed a new separation based label-free detection method that is capable of simultaneously detecting multiple proteins interacting with the same ligand on SLBs. Each protein moved the fluorescent biomarker to a different position in charged SLB under proper experimental conditions, and non-specific protein adsorption

did not give rise to any signals. Both free ligand and protein bound ligand concentrations were obtained, and the fluorescent intensity of each component was self-normalized.

Low concentrations of protein can be detected in the presence of interfering proteins and high concentrations BSA.

Competitive binding of Streptavidin and goat anti biotin was successfully investigated. It was found that the inhibition of goat anti biotin binding on biotin-cap-NBDPE by Streptavidin was more pronounced at lower goat anti biotin concentration. In principle, single proteins bound on SLBs could be detected when higher quantum yield fluorophores are used. In the future, any ligands of interest can be linked to fluorescently labeled phosphatidylethanolamine (PE) lipids through standard primary amine-carboxylic acid reaction. Multiple ligands could also be tested in one experiment, when they are linked to PE lipids with different fluorophores. Fluorescent membrane proteins can also be used in studying protein-protein interactions on SLBs. This method has a potential to become a high-throughput label-free detection method with high sensitivity and selectivity.

CHAPTER IV  
LABEL-FREE DETECTION OF ENZYME REACTION  
ON SUPPORTED LIPID BILAYER IN SITU

**Introduction**

Phospholipids play an important role in many important biological processes in cells, such as protein binding, intracellular signaling, apoptosis and biomolecule synthesis.<sup>72-76</sup> Different phospholipids and fatty acids are inter-convertible between each other through various enzymatic reactions on lipid membrane.<sup>76</sup> Phosphatidic acid (PA) accounts for 1-4% of the total lipids in eukaryotic cells.<sup>77</sup> PA is a central lipid in signaling reactions and works as a precursor for the biosynthesis of many other lipids.<sup>76,78-80</sup> PA also has key functions in regulating membrane curvature and vesicle fusion processes.<sup>72,80-83</sup> Phospholipase D (PLD) is the enzyme that catalyzes the hydrolysis of phosphatidylcholine (PC) to form phosphatidic acid (PA) and is activated by  $\text{Ca}^{2+}$  (**Figure 27**).<sup>84,85</sup> It is the enzyme linked to intracellular signal transduction, cancer, and other PA related functions.<sup>80</sup> A ping-pong-like ordered binding mechanism has been proposed for PLD. PC binds with PLD, and is converted into a covalent PA-PLD complex with the release of choline. The P-O bond between PA and PLD is then cleaved by nucleophilic attack of water on distal phosphate ester.<sup>86</sup> Real time AFM measurements also demonstrated that phospholipase D does not stay on the SLB surface after the reaction.<sup>87</sup>

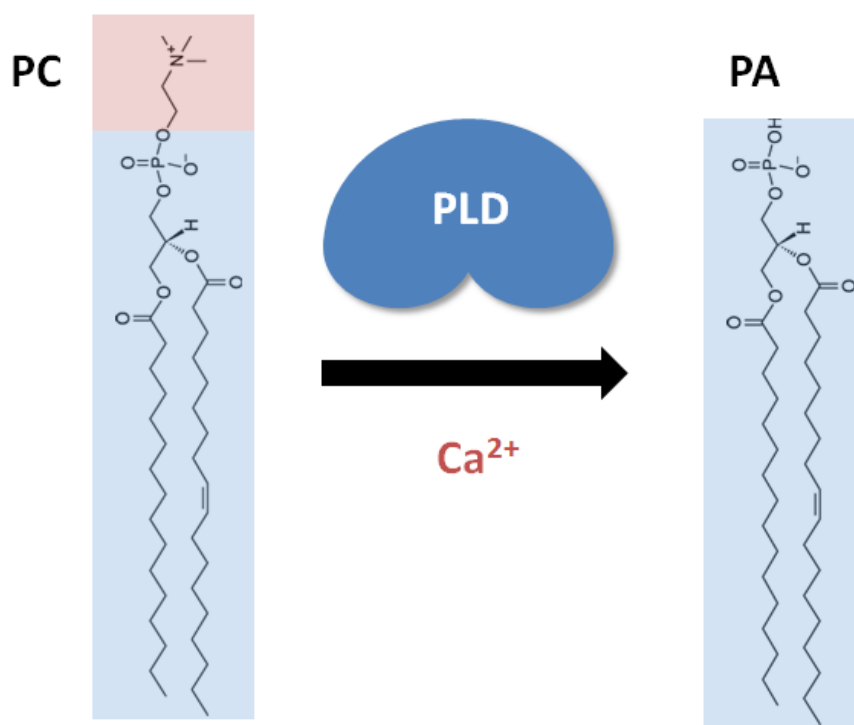


**Figure 27.** Illustration of Phospholipase D Catalyzed Lipid Hydrolysis.

Usually, enzymatic reactions on phospholipids are not monitored directly by measuring the concentration of the products. In the conventional method, phospholipase D activity is monitored by measuring the concentration of free choline released from PC using two-step chromogenic assay or using isotopically labeled choline.<sup>84,88-91</sup> In chromogenic assays, the released choline is first transformed into betaine and  $\text{H}_2\text{O}_2$  by choline oxidase. With 4-aminoantipyrine and sodium 2-hydroxy-3,5-dichlorobenzenesulfonate,  $\text{H}_2\text{O}_2$  then produces quinone dye in the presence of peroxidase. The concentration of the quinone dye is determined by measuring its absorbance around 500 nm.<sup>84,89,90</sup> The concentration of choline is not determined directly,



and the successive experiments may introduce extra fluctuations and errors into the results. The concentration of the biologically relevant product, PA, is rarely determined, simply because PA is a part of most phospholipids and has no characteristic absorption peaks. As a consequence, it is difficult to directly monitor PLD catalyzed PC to PA conversion on lipid membranes *in situ*.

Herein, we report a label-free method that can directly determine the percentage of PA on SLBs by observing the electrophoretic-electroosmotic focusing (EEF) position change of the fluorescent biomarkers.<sup>92</sup> On SLBs containing negatively charged lipids, negatively charged membrane-bound proteins were focused by the counteracting electrophoretic force and electroosmotic force. At the focusing position, the electrophoretic force and electroosmotic force on membrane-bound proteins should cancel each other. At this point, the zeta potential of the focused protein should be equal to the local surface zeta potential of the focusing position, which is directly related to the local surface charge density. Here, the membrane-bound protein works as an indicator for surface charge density. In an electric field parallel to the SLB, negatively charged lipids spontaneously build up a concentration gradient, generating higher negative surface charge density near the positive electrode. The mole percentage of negatively charged lipids is one of the factors that affect the focusing position of the protein, because it determines the distribution of surface negative charge density gradient. Under neutral pH value, PC is uncharged (zwitterionic) and PA is negatively charged. Thus, the PLD enzymatic reaction gives rise to the increase of the surface negative charge density

on SLB followed by the change of the focusing position of the fluorescent membrane-bound protein in EEF experiment (**Figure 28**).

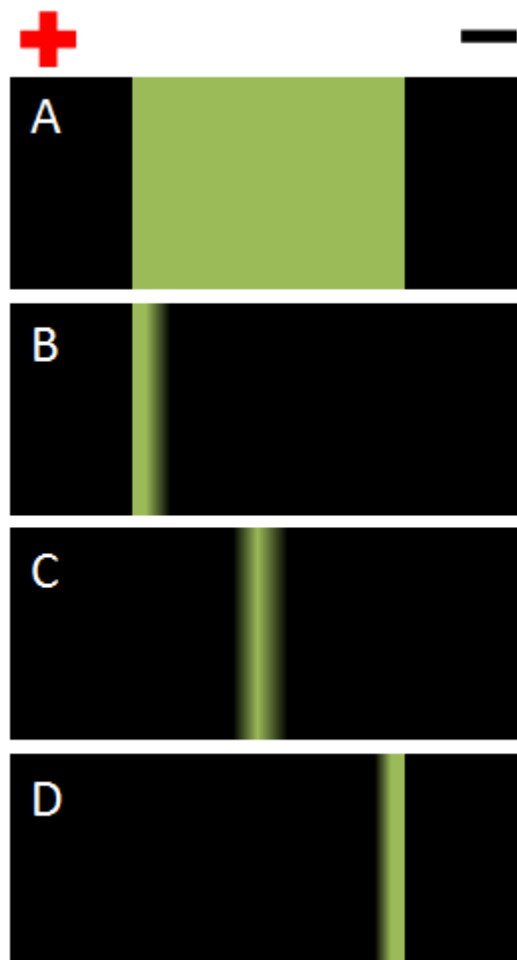


**Figure 28.** Schematic Diagram of Biomarker Focusing Position Change. StrA-4 biomarker focusing positions should be moved with increasing PA concentrations (from B to D). Initially, StrA-4 biomarkers are uniformly distributed on the entire SLB (A). The more PA forms, the boarder the negative charge density gradient is. Thus, the focusing position of StrA-4 is moved from the positive electrode side to the negative electrode side with increasing PA concentration.

## Experimental Section

### Materials

Fibrinogen and streptavidin were purchased from Sigma (St. Louis, MO). 1-palmitoyl-2-oleoyl-*sn*-glycero-3-phosphocholine (POPC), 1,2dioleoyl-*sn*-glycero-3-phosphoethanolamine-*N*-(cap biotiny) (biotin-cap-DOPE), and 1-palmitoyl-2-oleoyl-*sn*-glycero-3-phosphate (POPA) were purchased from Avanti Polar Lipids (Alabaster, AL). 1,2-dihexadecanoyl-*sn*-glycero-3-phosphoethanolamine-*N*-Texas Red (TXR-DHPE) was purchased from Invitrogen (Grand Island, NY). Polydimethylsiloxane (PDMS) was obtained from Dow Corning (Sylgard, silicone elastomer-184). Phospholipase D was purchased from Enzo Life Sciences (Farmingdale, NY).

### SLB Formation

In the following experiments, Alexa-488 labeled Streptavidin (StrA) was used as fluorescent biomarker. The patterned SLBs were formed by vesicle fusion on patterned glass slides.<sup>7,21,92</sup> Each SLB patch was about 400  $\mu\text{m}$  wide. Flow cell electrophoresis device was used to make the experimental conditions constant.<sup>29</sup> The SLB was composed of 99.4% POPC, 0.5% biotin-cap-DOPE and 0.1% TXR-DHPE. Biotin-cap-DOPE provided binding sites for StrA. TXR-DHPE was added to ensure the formation of good SLB, and also could be used as a second biomarker which indicated the distribution of the surface negative charge density gradient.

### Phospholipase D (PLD) Reaction on Supported Lipid Bilayers

10 mM pH 7.5 Tris buffer with 0 mM, 2.5 mM, 5 mM and 10 mM  $\text{CaCl}_2$  were used to dilute 25 kU/mL PLD stock solution. After the formation of patterned SLBs, 100  $\mu\text{L}$  1.4 U/mL PLD solution with different  $\text{Ca}^{2+}$  concentrations were incubated on SLBs at room temperature, and rinsed off using 30 mM EDTA Tris buffer. After the reaction, 5 nM Alexa-488 labeled Streptavidin solution (in 10mM Tris, pH 7.5) was incubated with the SLBs for 30 minutes, and rinsed off using 10 mM Tris buffer. EEF experiments were done in pH 7.5 10 mM Tris buffer and 50 V/cm electric field.

### Results and Discussion

Before the PLD activity assay, the behavior of TXR-DHPE and StrA on SLBs were investigated. After the formation of SLBs containing 0.1% TXR-DHPE, 5 nM Alexa-488 labeled Streptavidin in 10mM pH 7.5 Tris buffer was added onto the SLB and incubated for 30 minutes. Then the bulk proteins were rinsed off using 10 mM Tris buffer. Initially, both StrA and TXR-DHPE were uniformly distributed on the SLB (**Figure 29**). After the application of 50 V/cm electric field for 45 minutes, TXR-DHPE accumulated on the positive electrode edge of the SLB (**Figure 29**), simply due to the electrophoretic force on the negative charge of TXR-DHPE. StrA also formed a narrow band very close to the positive electrode edge. TXR-DHPE and Biotin-cap-DOPE were negatively charged and contributed a small surface charge density gradient, so that StrA was not focused exactly on the edge.

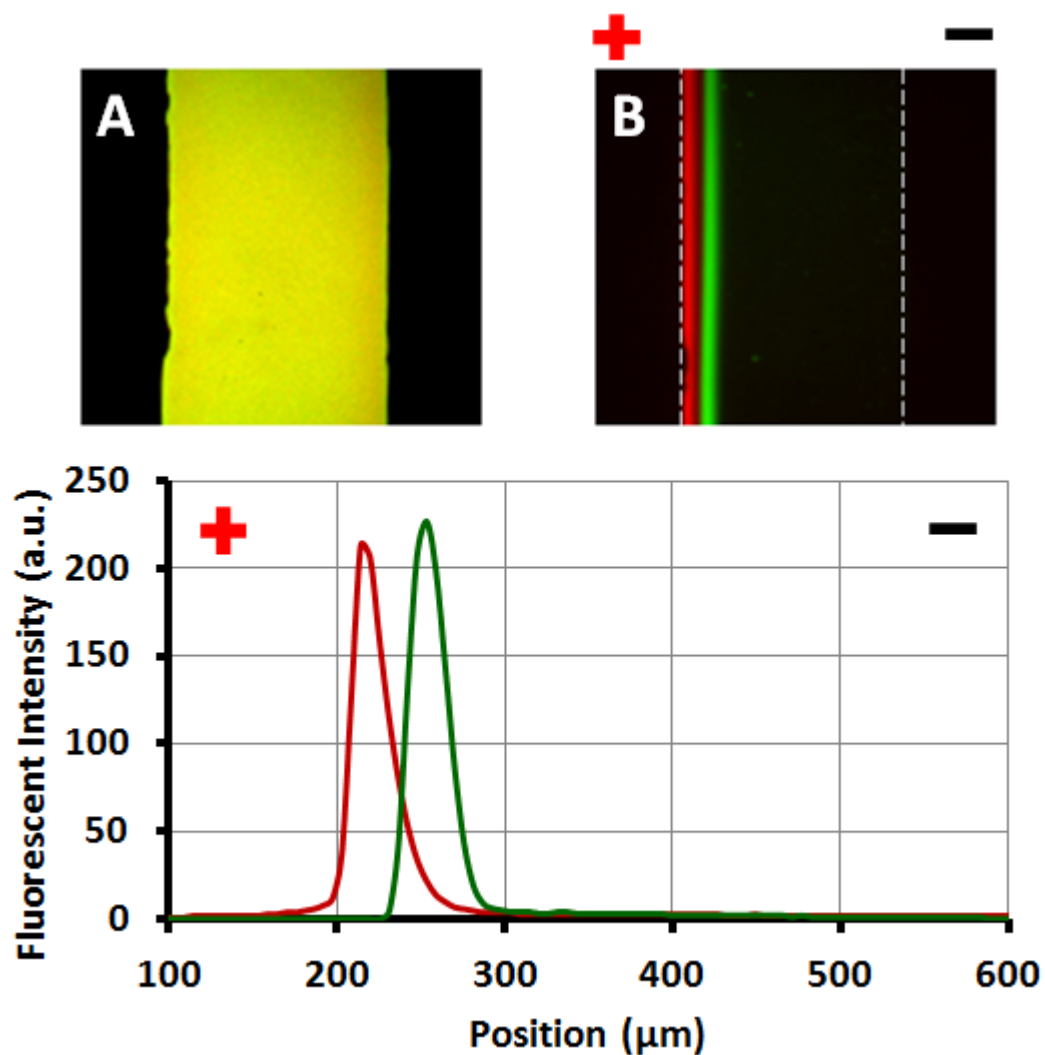


**Figure 29.** Focusing of Biomarkers without Reaction. Fluorescence images of StrA (green) on SLB containing 0.1% TXR-DHPE (red), 0.5 % biotin-cap-DOPE and 99.4 % POPC before (A) and after (B) electrophoretic-electroosmotic focusing (EEF) experiment in 50 V/cm electric field for 45 minutes. Initially, StrA and TXR-DHPE were uniformly distributed on the entire SLB. The line-scan profile of StrA and TXR-DHPE after EEF was shown on the bottom.

Next, we looked at PLD activity on SLBs with the same composition as in the last experiment. Because  $\text{Ca}^{2+}$  is one of the activators of PLD<sup>85,90</sup>, the PA conversion rates were measured in four different  $\text{Ca}^{2+}$  concentrations. 10 mM pH 7.5 Tris buffer with 0 mM, 2.5 mM, 5 mM and 10 mM  $\text{CaCl}_2$  were used to dilute 25 kU/mL PLD stock solution. After the formation of patterned SLBs, 100  $\mu\text{L}$  1.4 U/mL PLD solution with different  $\text{Ca}^{2+}$  concentrations were incubated on SLBs for 10 minutes at room temperature, and rinsed off using 30 mM EDTA Tris buffer. As shown in **Figure 30**, StrA were focused near the positive electrode side of the SLB in 0 mM  $\text{Ca}^{2+}$ . Compared to StrA on SLBs without PLD incubation, the focusing position was not changed obviously. Without  $\text{Ca}^{2+}$ , PLD should have no catalytic activity, therefore no PA lipids were produced and the focusing position of StrA should not be changed. Then 2.5 mM, 5 mM and 10 mM  $\text{Ca}^{2+}$  concentrations were used. In this  $\text{Ca}^{2+}$  concentration range, PLD activity should increase almost linearly.<sup>90</sup> Thus, the amount of PA in SLBs should be proportional to the concentration of  $\text{Ca}^{2+}$ , when the SLBs were incubated with PLD and  $\text{Ca}^{2+}$  for the same period of time. In 2.5 mM  $\text{Ca}^{2+}$ , the StrA band finally stopped at the position about 100  $\mu\text{m}$  away from the positive electrode edge of the SLB (**Figure 30**). The negative charge density should be the same at the focusing position of StrA.

Therefore, the result indicated that a broad negative charge density gradient was formed and thus more negatively charged lipids (PA) were produced. Based on **Eq. 6**, the percentage of PA was calculated to be about 8%. In 5 mM  $\text{Ca}^{2+}$ , the StrA band stopped at the position about 300  $\mu\text{m}$  away from the positive electrode edge of the SLB (**Figure 30**), indicating that more negatively charged lipids (PA) were produced than in 2.5 mM  $\text{Ca}^{2+}$ . The percentage of PA was calculated to be about 15%. In 10 mM  $\text{Ca}^{2+}$ , the StrA band was pushed all the way to the negative electrode edge of the SLB (**Figure 30**). The concentration of negatively charged PA was so high that the electroosmotic force on StrA at any point on the SLB was much larger than the electrophoretic force on StrA. In this condition, the percentage of PA was too high to be determined, and the PA percentage should be higher than 25%. Because all SLBs had the same width and the experimental conditions were the same, the line-scan profiles of StrA in 0 mM, 2.5 mM, 5 mM and 10 mM  $\text{Ca}^{2+}$  were overlaid. Clearly, the StrA band gradually moved from the positive electrode side to the negative electrode side with increasing  $\text{Ca}^{2+}$  concentration (**Figure 30, 31**).

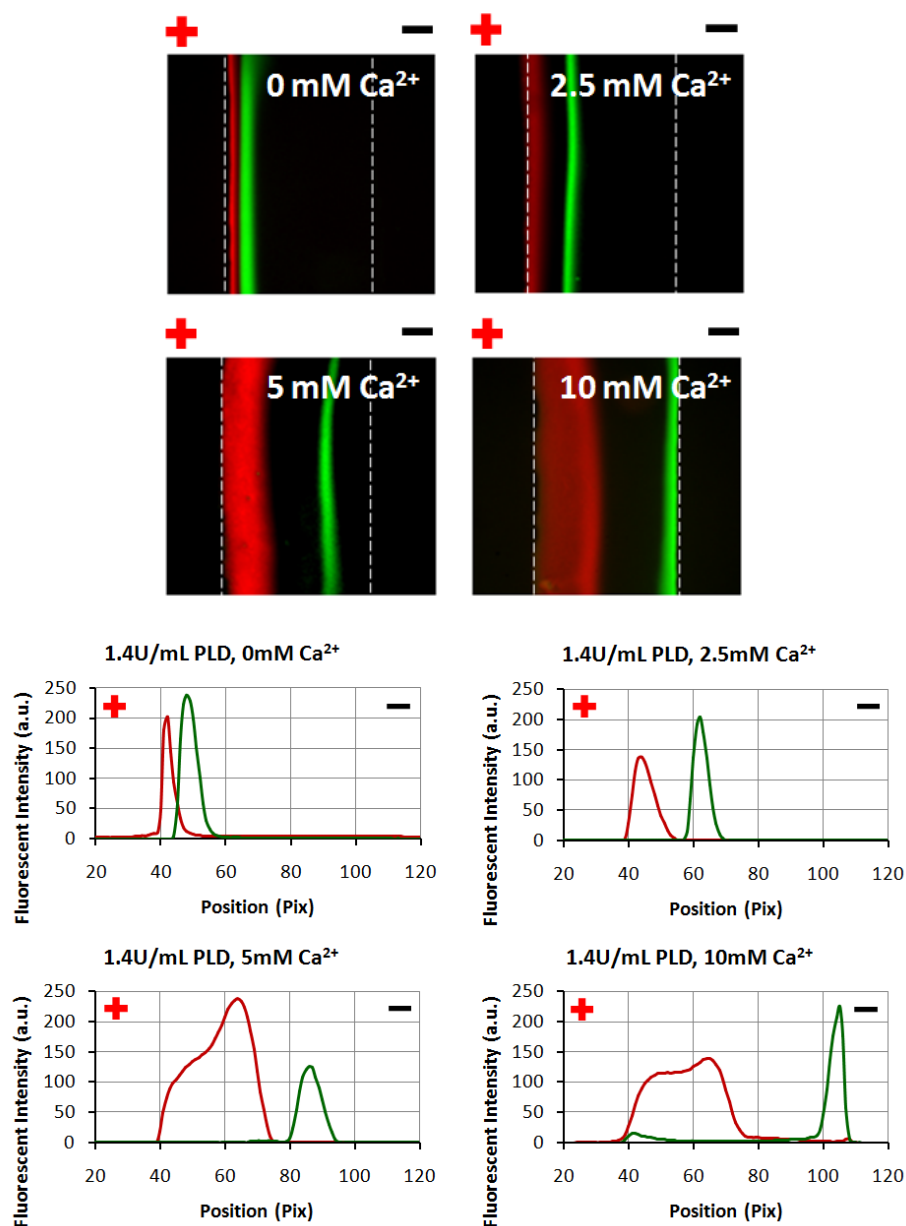


**Figure 30.** Focusing of Biomarkers in Different Conditions. Electrophoretic-electroosmotic focusing (EEF) of TXR-DHPE lipids and StrA-4 biomarkers on SLBs after PLD catalyzed reaction in different concentration of  $\text{Ca}^{2+}$ . SLBs were incubated with PLD and  $\text{Ca}^{2+}$  for 10 minutes. The corresponding line-scan profiles are on the bottom.



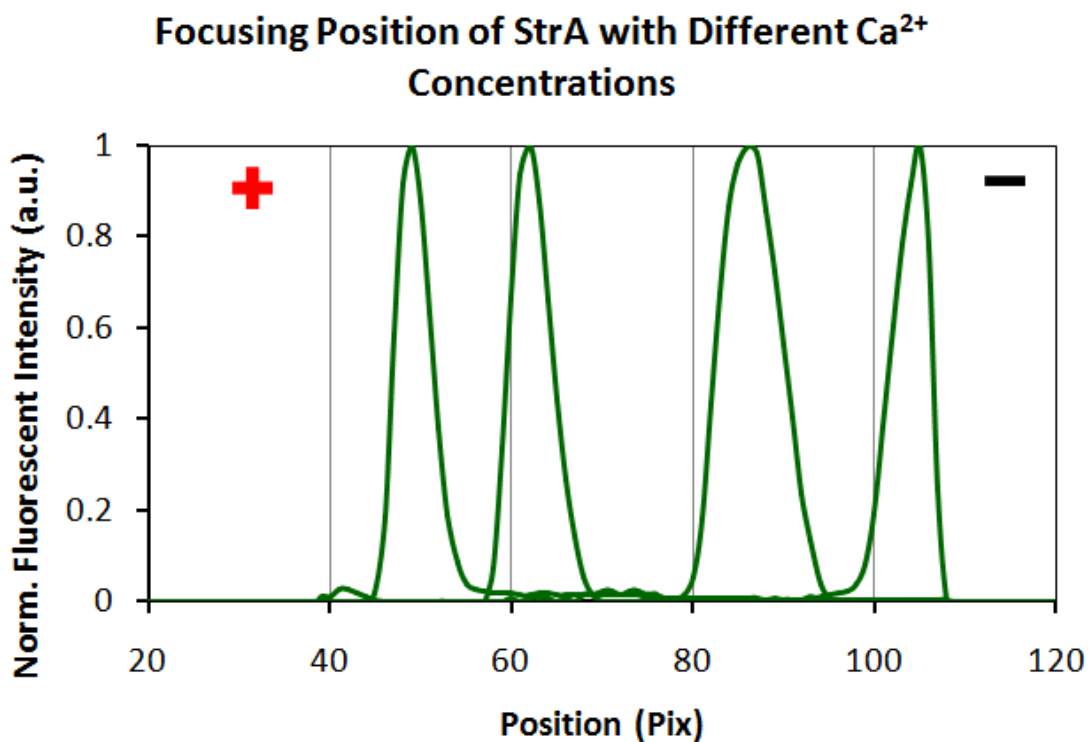


**Figure 31.** Comparison of Biomarker Focusing Positions in Different Conditions. Line-scan profiles of StrA-4 biomarker focusing positions on SLBs after PLD catalyzed reaction in 0 mM, 2.5 mM, 5 mM and 10 mM of Ca<sup>2+</sup> (From left to right) are overlapped. All SLBs were incubated with PLD and Ca<sup>2+</sup> for 10 minutes. Because all SLBs had the same width, so the line-scan profiles could be combined and compared directly.

At the same time, the width of TXR-DHPE band was also affected by the formation of PA. The higher the PA mole percentage, the wider the TXR-DHPE band was. And it was interesting that TXR-DHPE spread over the high PA percentage region and formed a peak away from the edge of the SLB (**Figure 30**). There may be two

reasons, first, TXR-DHPE and PA were de-mixed in electric field;<sup>8</sup> second, TXR-DHPE also experienced small electroosmotic force because of its large head group.<sup>92</sup>

The focusing kinetics of StrA was also affected obviously by the formation of high percentage of PA. Without PA formed, StrAs were driven by the electrophoretic force and moved continuously to the positive electrode side edge of SLBs (**Figure 32**). In the experiment with 5 mM  $\text{Ca}^{2+}$ , where about 15% PA was produced, StrA was pushed to the negative electrode side by strong electroosmotic force in the beginning, and then moved backwards (to the positive electrode side) while PA was depleted on the negative electrode side. After formation and stabilization of PA gradient, StrA finally was focused and stopped in the middle of the SLB (**Figure 32**).

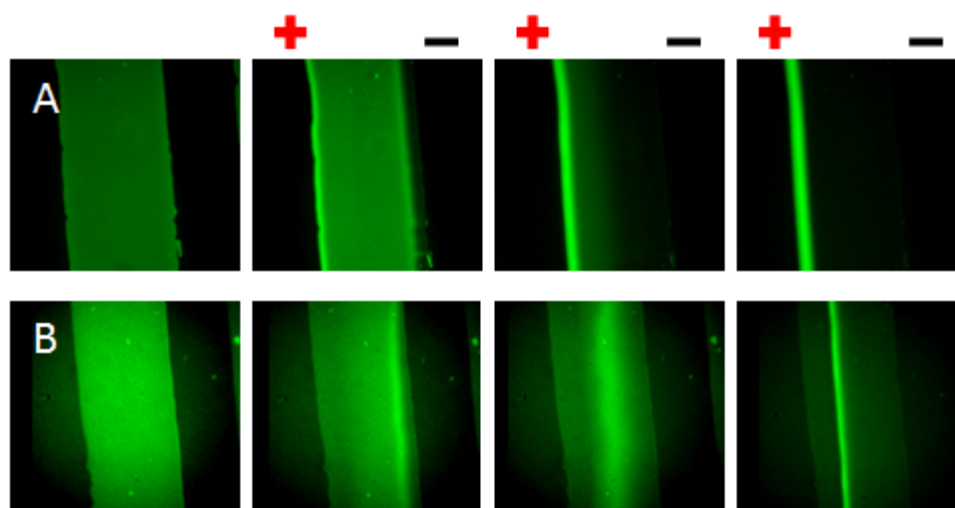


**Figure 32.** Migration Kinetics of Biomarkers in Different Conditions. Migration of StrA-4 was monitored in SLB (A) without PA formation (B) with PA formation.

In order to prove the formation of phosphatidic acid (PA) in SLBs, matrix-assisted laser desorption/ionization (MALDI) mass spectrum of the lipids after PLD reaction was also taken. After the reaction, SLBs were frozen by liquid nitrogen, and then vacuumed for 4 hours to remove the water molecules. Then the dried lipids sample was re-dissolved in 50% acetonitrile and 50% methanol solvent containing 10 mg/mL  $\alpha$ -cyano-4-hydroxycinnamic acid (matrix). 2  $\mu$ L solution was then dipped on metal plate, and the solvent was then evaporated. The molecular mass of negatively charged POPA lipids, which were hydrolyzed from POPC, should be 674, and the molecular mass of POPA-Na should be 696 (**Figure 33**).

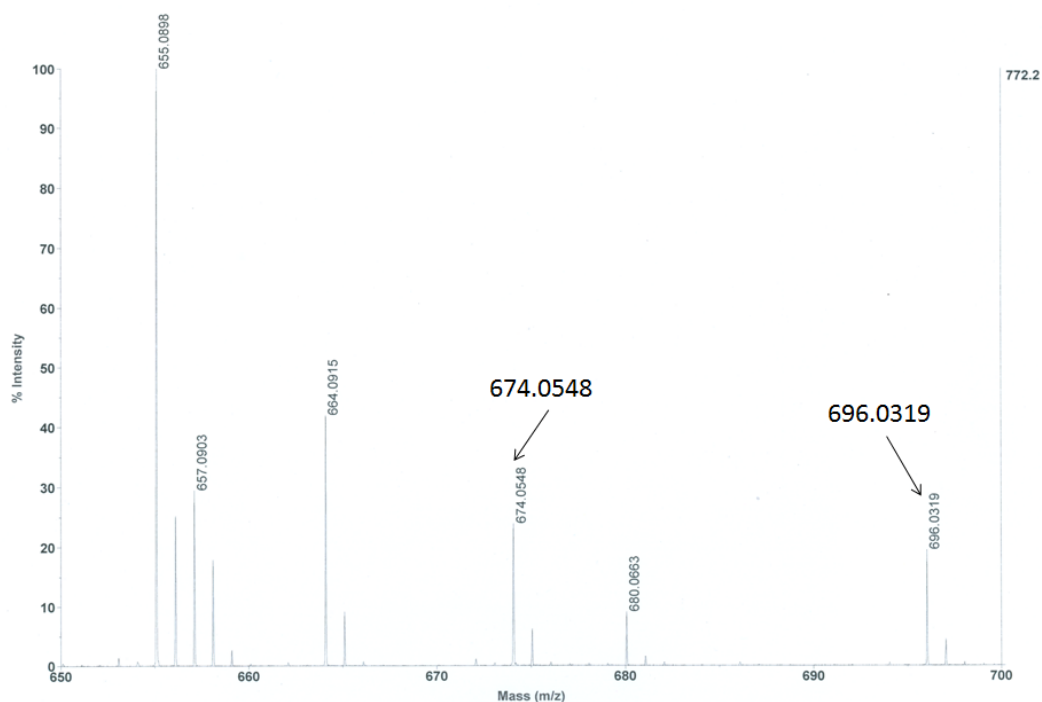


**Figure 33.** Mass Spectrum of Phosphatidic Acid Product. The MALDI mass spectrum of SLB was taken after PLD catalyzed PC to PA conversion. PA molecular ion peak showed at  $m/z$  674.0548, and PA-Na peak showed at  $m/z$  696.0319.

The effect of PA on the focusing position of StrA on SLBs was also investigated in exactly the same EEF experimental conditions as above. POPA was mixed in SLBs beforehand, and 5% and 10% POPA mole percentages were used. Compared to SLBs without POPA, 10% POPA gave rise to a dramatic shift of StrA focusing position, while 5% POPA did not affect StrA focusing position (**Figure 34**). Therefore, the formation of POPA could be detected when its concentration was higher than 5%.

## Conclusions

In conclusion, we developed a new *in situ* label-free detection method for lipids enzymatic reaction by monitoring the focusing position change of fluorescently labeled biomarkers. Compared to the conventional method, the concentration of lipid product was determined directly and no successive experiments needs to be done. The PLD enzyme reaction on SLBs required much less materials than in bulk. After the detection, the SLB can be restored to its original state when turning off the electric field. In future, other enzymatic reactions that involve the change of charges on lipids can be monitored label-freely in a similar way, such as phosphorylation, de-phosphorylation, lipid biosynthesis and other phospholipase reactions.

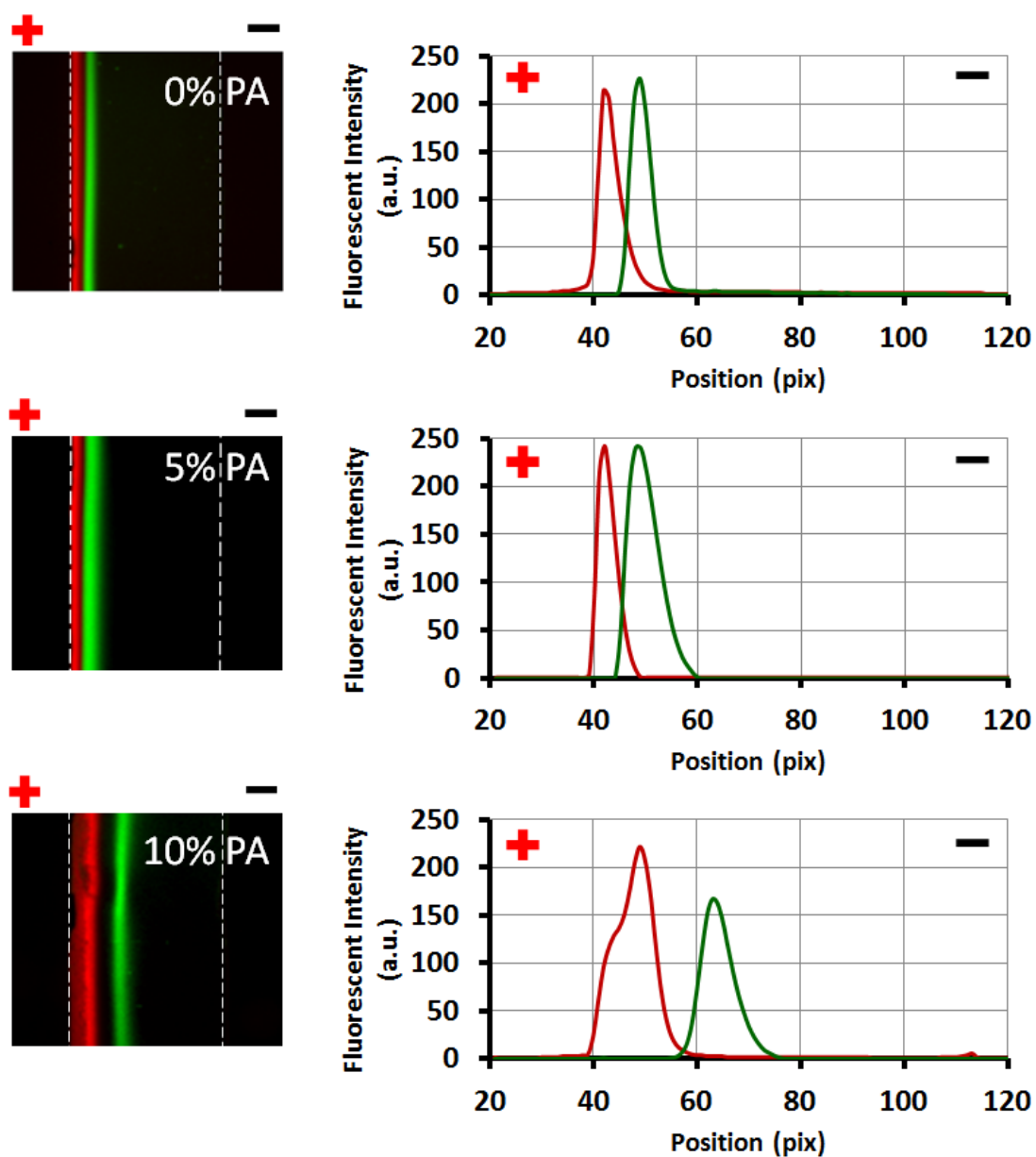


**Figure 34.** Effect of Phosphatidic Acid on Biomarker Focusing Position. StrA-4 was moved away from the positive electrode edge of the SLB with increased percentage of PA mixed in the SLB.

## CHAPTER V

### COMPARTMENTALIZATION OF SUPPORTED LIPID BILAYER USING MAGNETIC PARTICLES

#### **Introduction**

Membrane-associated proteins and lipids have been successfully separated and enriched by several different methods on SLBs, such as electrophoresis, surface acoustic wave and laminar flow.<sup>12,13,35,39,92</sup> It can be expected that further experiments could be done directly on the purified proteins or lipids on SLBs, such as cell-membrane interactions, protein-membrane interactions and protein-receptor interactions. However, the concentrated charged molecules will diffuse and re-mix quickly when the external electric field or mechanical flow is turned off. Therefore, post-separation treatments have to be done to rapidly stop the diffusion of separated species under physiological conditions. Additionally, the post-separation treatments have to keep the majority of materials on the surface and avoid the use of chemical reactions, which could potentially affect the function and structure of proteins and lipids. Thus, physical methods are more favorable. If the whole SLB broken into many small pieces, there should not be any diffusion between individual pieces and the separated species can be preserved.

In the past, several methods have been developed to produce discontinuous SLB patterns.<sup>10,21-28</sup> Basically, two strategies were applied to make patterned SLBs. First, a large and uniformed SLB was formed on the surface, then physical barriers were

produced by eliminating patterned lipid bilayer structures, such as mechanical scratching, PDMS stamping and UV radiation.<sup>10,21,23,28</sup> Second, physical barriers were patterned on the surface before SLB formation by lithography, stamping or laminar flow.<sup>10,22,24-27</sup> The post-separation treatment should utilize the techniques in the first category, because the continuous SLB used in separation has to be broken down into many small pieces. However, previously developed methods cannot meet the requirements mentioned above, either due to long process time or removal of a lot of materials.

Here we propose a “differentiation method” using magnetic particles to rapidly slice the whole SLB into many small patches after electrophoretic separation. As illustrated in **Figure 35**, magnetic particles are first introduced into solution. With the application of an external magnet below the glass slides on which the SLB was formed, magnetic particles penetrate through the SLB and have direct contacts with the glass surface. Holes on the SLB are generated by the contact spots between the particles and glass surface. Even if the particles are closely packed, there must be large spaces between the holes on SLB. Then the external magnet is moved back and forth on the direction that was perpendicular to the separation direction, and the whole SLB should be sliced into many small pieces by the movement of magnetic particles. Bare glass surface should be exposed by the movement tracks of magnetic particles,. This process should take very short time. Afterwards, to prevent the recombination of SLB slices, BSA can be used to fill the gaps between SLB pieces, so that permanent physical barriers are formed. Finally, the magnet below the glass slide is removed and magnetic

particles can also be removed from solution by another magnet on top of the bulk solution.

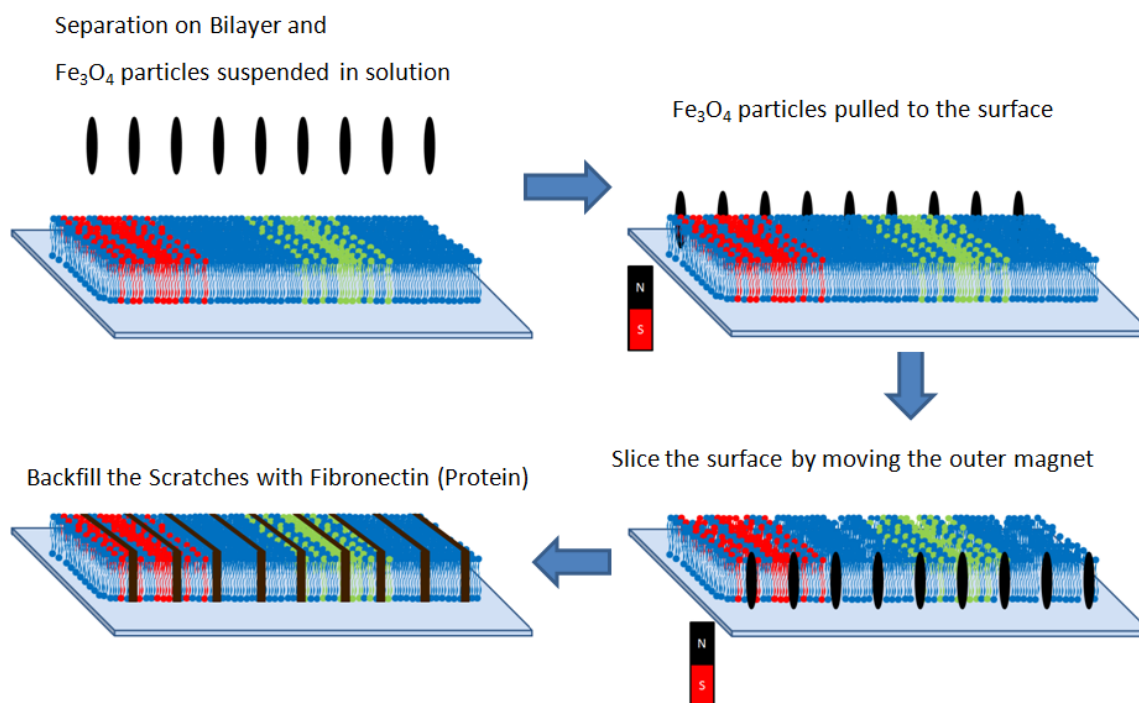


**Figure 35.** Compartmentalization of SLBs Using Magnetic Particles. Magnetic particles were pulled through the SLB by external magnet under the glass slide. The movement of magnetic particles can divide the continuous SLB into many small pieces.

## Experiments and Results

In the beginning, we made a test to look at whether scratches could be made by the movement of magnetic particles on SLBs. The SLB was composed of 99% POPC and 1% fluorescently labeled NBDPC, and was formed by vesicle fusion method on



glass slide.<sup>7</sup> A fluorescent microscope was used to observe the SLB. As shown in **Figure 36**, scratches were made by the movement of a few magnetic particles on SLB surface. The dark lines on SLB originated from the removal of fluorescently labeled lipids, which in turn indicated the removal of lipid bilayer structure. From the line-scan profile, the widths of most scratches were less than 1  $\mu\text{m}$ , which was one order of magnitude narrower than the previously reported patterning methods, except AFM lithography.<sup>23,26</sup> Also, it only took seconds to make these scratches, which is a lot faster compared to other methods.<sup>10,21-28</sup>

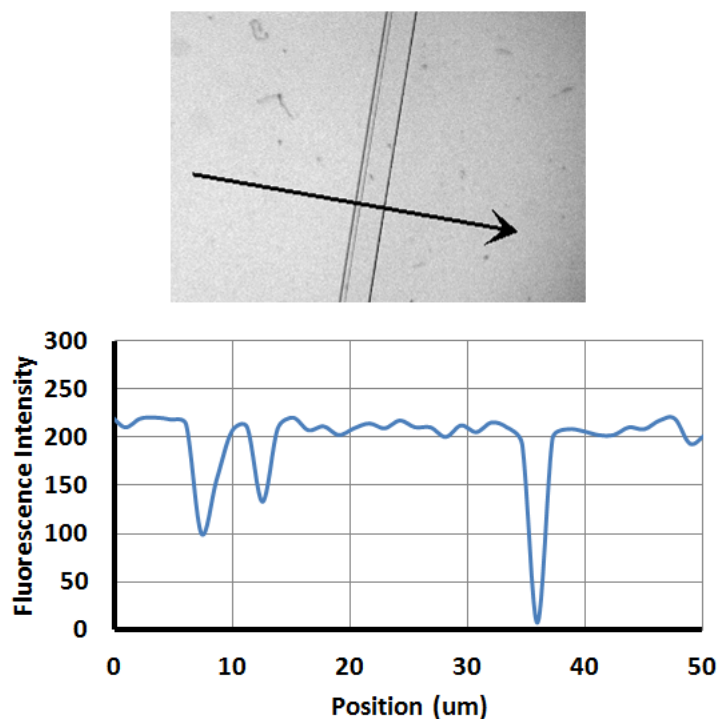


**Figure 36.** Scratching SLBs Using Magnetic Particles. Fluorescence image and line-scan profile of scratches produced by magnetic particle scratching are shown. The SLB contains fluorescently labeled lipids, and the dark lines are the scratches.

To look at the mobility of SLB after magnetic particle scratching, Fluorescent Recovery After Photobleaching (FRAP) measurements were also made. Fluorescent NBDPC were bleached by intensive radiation at 488 nm wavelength. Because the SLB was two dimensional fluid, the bleached NBDPC could diffuse out of the original bleached area and fluorescent NBDPC could diffuse into the bleached area. Therefore, without any barriers, the fluorescent intensity of the bleached area recovered after 20 minutes (**Figure 37A, D**). The introduction of physical barriers should definitely confine the two-dimensional fluidity of lipids. With the increasing amount of scratches, the fluorescent recovery gradually became slower (**Figure 37B, E**). Finally, when the continuous SLB was broken down into many patches that had much smaller area than the bleached region, no obvious FRAP was observed (**Figure 37C, F**). Because each SLB patch was completely surrounded by scratches and isolated from other patches, there was no lipid diffusion from one patch to another. For the SLB patches in the interior of the bleach region, all fluorescent lipids were bleached, so that there were no FRAP in those patches. For the SLB patches on the edge, part of the fluorescent lipids were bleached, so that there were partial FRAP on those patches. This proves that we have successfully made sub-micrometer size scratches on SLBs by magnetic particles and “differentiated” the continuous SLB into many small patches in several seconds.

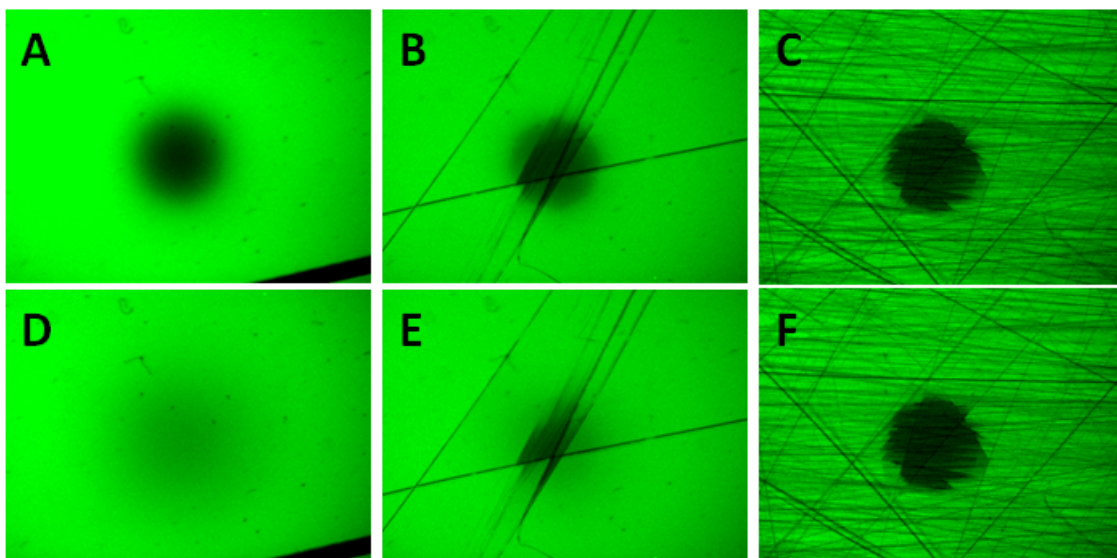


**Figure 37.** FRAP of SLBs with Different Amount of Scratches. (A), (B), (C) are fluorescent images right after photobleaching. (D), (E), (F) are fluorescent images 20 minutes after photobleaching. The SLB contains fluorescently labeled lipids, and the dark lines are the scratches.

Magnetic particles were also used to “differentiate” SLBs after electrophoretic-electroosmotic focusing (EEF) separation. In EEF experiment, membrane-bound proteins and lipids were separated on a 400  $\mu\text{m}$  wide SLB by the counter-acting electrophoretic force and electroosmotic force.<sup>92</sup> Three fluorescent components, NBD-DPPE, Alexa-488 labeled StrA and Alexa-594 labeled IgG anti biotin were concentrated and separated from each other in 50 V/cm electric field and 10 mM pH 7.0 Tris buffer (**Figure 38A**). The separation was given by a negative charge density gradient formed by the accumulation of negatively charged lipids.<sup>92</sup> In the final steady state, there were concentrated negatively charged analytes and a negative charge density gradient, so that

these concentrated negatively charged species should start to diffuse immediately after the cutting-off of external electric field. To preserve the separated species on SLB, magnetic particles were introduced to solution right after the electric field was turned off. Larger amount of magnetic particles were used to “differentiate” a larger area at one time. In **Figure 38B**, the 400  $\mu\text{m}$  wide SLB was “differentiated” after the separation of three species, and incubated with 5 mg/mL BSA solution for 30 minutes. From the fluorescent image and the line-scan profile, the separated species were kept at nearly the same positions as the positions in electric field. Due to the strong physical barriers formed by BSA adsorption on exposed bare glass surface, the separated species on the SLB could be kept for at least 48 hours. In the fluorescent images, it could be seen that the widths of magnetic particle scratches were much narrower than the width of the SLB. Thus, only a small amount of materials was removed by magnetic particle scratching. The diffusion of separated species on SLBs could be constrained by freezing the SLBs immediately in liquid nitrogen. However, no further experiments could be conducted on SLBs under physiological conditions any more. Now, compartmentalization of SLBs using magnetic particles also provides a simple solution to break through this limitation.

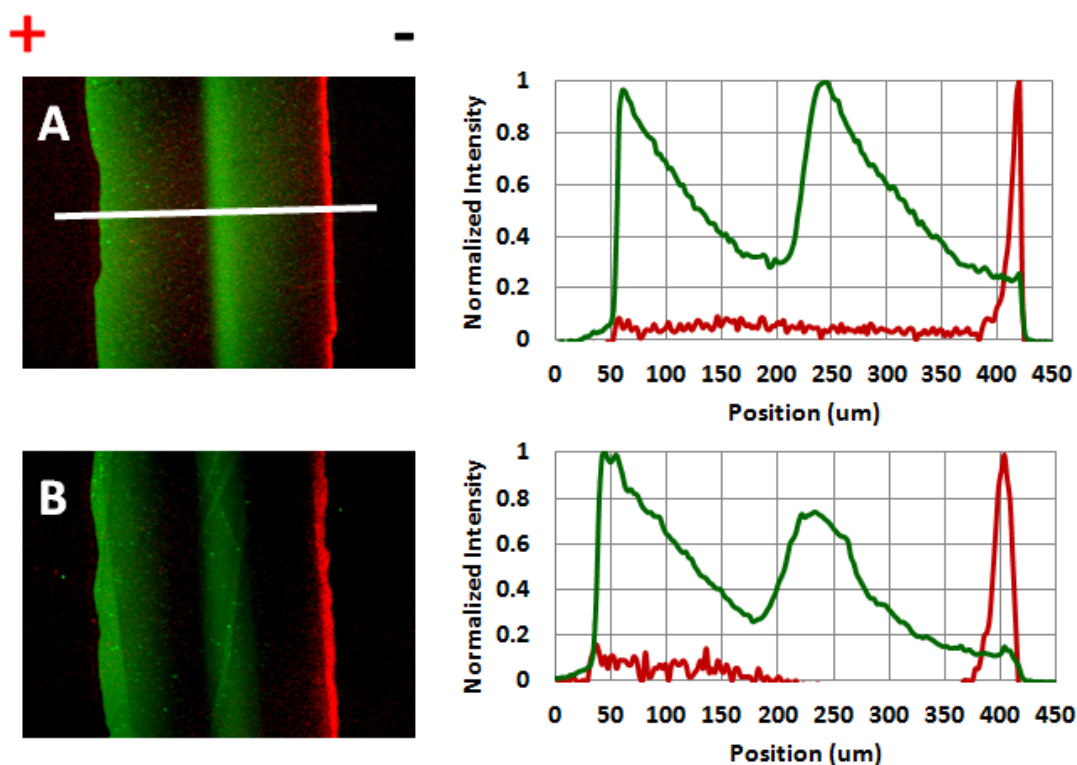


**Figure 38.** Preservation of Separation Using Magnetic Particle Scratching. (A) EEF separation of membrane-bound proteins and lipids. (B) Preservation of separated peaks using magnetic particle scratching, and the image was taken 24 hours after separation. The corresponding line-scan profiles are on the right of each image.

Furthermore, SLB differentiation using magnetic particles was also found to be a useful method to preserve biomolecule concentration gradients generated from uniformed SLBs in electric field. Large scale SLB arrays with variations in composition could be used as high-throughput tools to study protein-ligand and protein-membrane interactions.<sup>27,93-95</sup> SLB differentiation by magnetic particles actually could provide SLB patches with more continuous compositional variation compared to the previous

methods. Biotinylated NBDE (biotin-cap-NBDPE) was a fluorescent phospholipid with one negative charge on the phosphate group at neutral pH (**Figure 14**). The biotin functional group was linked to the primary amine group on the hydrophilic head of fluorescent NBDPE through carboxylic acid and amine reaction. SLBs with 1% biotin-cap-NBDPE and 99% POPC were formed on glass slides using the vesicle fusion method. A fluorescent microscope was used to observe the SLB, and all fluorescence signals came from biotin-cap-NBDPE lipids. Initially, biotin-cap-NBDPE lipids were uniformly distributed in the entire SLB. The application of 10 V/cm electric field parallel to the SLB gave rise to the migration of negatively charged biotin-cap-NBDPE lipids towards the positive electrode. Finally, together with the thermal broadening effect and electrostatic repulsion between negative charges,<sup>8</sup> a stable biotin-cap-NBDPE gradient was formed across the SLB, with higher biotin-cap-NBDPE density near the positive electrode side on the SLB (**Figure 38**). After the electric field was turned off, the SLB was differentiated by magnetic particles and BSA was used to create permanent physical barriers. In **Figure 38**, it was obvious that the fluorescence gradient was preserved on the SLB after magnetic particle scratching. Thus, biotin-cap-NBDPE gradient should also be created. To prove the formation of biotin gradient on the SLB, Alexa-594 labeled Streptavidin (StrA) was then added to solution and incubated with the SLB for 30 minutes. Then bulk StrAs were rinsed off using 10 mM Tris buffer. Both biotin-cap-NBDPE fluorescence and StrA fluorescence were monitored. According to the line-scan profiles (**Figure 39**), the fluorescent intensity of StrA on SLB surface increased as the fluorescent intensity of biotin-cap-NBDPE increased. The fluorescence

intensity of StrA was plotted against the fluorescence intensity of biotin-cap-NBDPE, and a very good linear relationship was obtained (**Figure 40**). In the fluorescent images, it should also be noticed that the widths of magnetic particle scratches were so narrow that it was nearly not observable under a 10X objective.

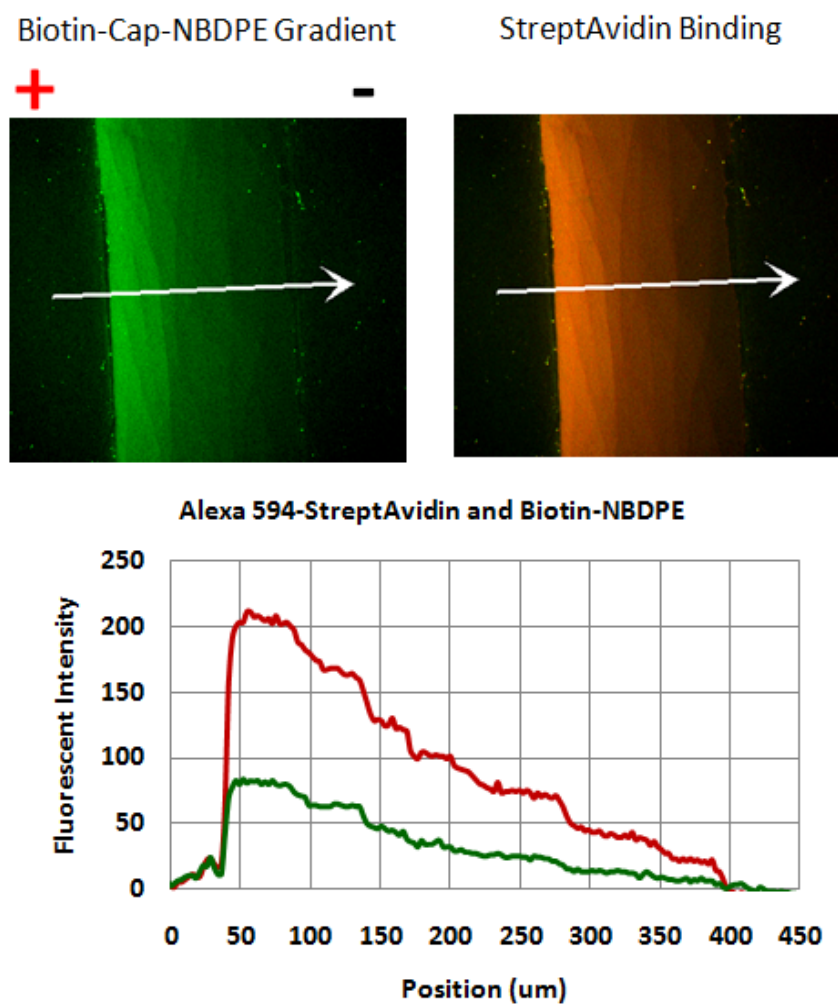


**Figure 39.** Preservation of Lipid and Protein Gradients. Biotin-cap-NBDPE lipids gradient and Streptavidin gradient were formed and preserved on SLB. The corresponding line-scan profiles of biotin-cap-NBDPE (green) and Streptavidin (Red) are on the bottom.

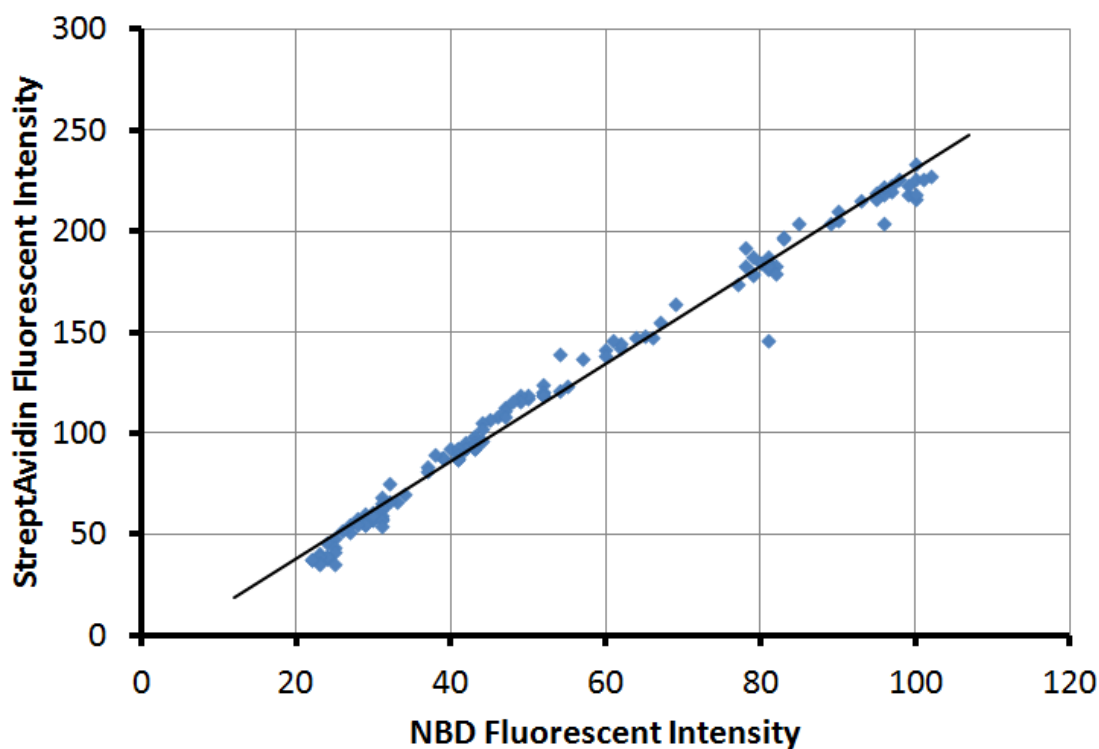


**Figure 40.** Relationship between Biotin-cap-NBDPE Fluorescent Intensity and Streptavidin Fluorescent Intensity. The data were obtained from the line-scan profile of the SLB in **Figure 39**. A good linear relationship was obtained.

## Conclusions

In conclusion, magnetic particles were successfully used to make scratches on SLBs. Using magnetic particles, continuous SLBs were broken down into many small SLB pieces within a very short time, while most material on the SLBs were kept intact. Diffusion of membrane associated biomolecules was confined by the physical barriers formed by BSA on the scratches. This method has been successfully applied in



preserving separations and charged biomolecule gradients on SLBs under physiological conditions after the electric field was turned off. Because all experiments were done under physiological conditions, differentiated SLBs can be used for many further experiments, ranging from protein-SLB interactions to cellular level experiments.

## CHAPTER VI

### CONCLUSIONS

We developed a new electrophoretic-electroosmotic focusing (EEF) method that made use of the surface charge density gradient to separate and enrich proteins and lipids from homogeneous SLBs. EEF is ideally suited for work with systems containing trace membrane concentrations of membrane proteins. This method can be used to separate, accumulate and potentially identify many components in protein-lipid mixtures on charged SLBs. In order to preserve the separation on two dimensional fluidic SLB, magnetic particles were used to divide continuous SLBs into many small SLB pieces within a very short time, while most material on the SLBs were kept intact. Diffusion of membrane associated biomolecules was confined by the physical barriers formed by BSA on the scratches afterwards. This method was also successfully applied in preserving separated species and charged biomolecule gradients on SLBs under physiological conditions after the electric field was turned off.

Based on EEF, two label-free detection methods were also developed. The first one was label-free detection of protein competitive binding on the same kind of ligand on SLBs. It was based on the change of electrophoretic force and electroosmotic force on fluorescently labeled ligands caused by protein binding. Each protein moved the fluorescent biomarker to a different position in charged SLBs under proper experimental conditions, and non-specific protein adsorption cannot give rise to any signals. Low concentration of protein can be detected in the presence of interfering proteins and high

concentration of BSA. In future, ligands of interest can be linked to fluorescently labeled phosphatidylethanolamine (PE) lipids through the standard primary amine-carboxylic acid reaction. The second one is an *in situ* lipids enzymatic reaction label-free detection method by monitoring the change of focusing position of fluorescently labeled biomarkers. It was based on the surface charge density change caused by the enzyme reaction with POPC. After the detection, the SLB can be restored to its original state when turning off the electric field. In future, other enzymatic reactions that involve the change of charges on lipids can be monitored in a label-free fashion in a similar way, such as phosphorylation, de-phosphorylation, lipids biosynthesis and other phospholipase reactions.

## REFERENCES

- (1) Wong, A. P.; Groves, J. T. *Proc. Natl. Acad. Sci. U. S. A.* **2002**, *99*, 14147.
- (2) Holden, M. A.; Cremer, P. S. *Annu. Rev. Phys. Chem.* **2005**, *56*, 369.
- (3) Lou, C.; Wang, Z.; Wang, S.-W. *Langmuir* **2007**, *23*, 9752.
- (4) Shi, J. J.; Yang, T. L.; Kataoka, S.; Zhang, Y. J.; Diaz, A. J.; Cremer, P. S. *J. Am. Chem. Soc.* **2007**, *129*, 5954.
- (5) Hamai, C.; Cremer, P. S.; Musser, S. M. *Biophys. J.* **2007**, *92*, 1988.
- (6) Diaz, A. J.; Albertorio, F.; Daniel, S.; Cremer, P. S. *Langmuir* **2008**, *24*, 6820.
- (7) Brian, A. A.; McConnell, H. M. *Proc. Natl. Acad. Sci. U. S. A.* **1984**, *81*, 6159.
- (8) Groves, J. T.; Boxer, S. G.; McConnel, H. M. *Proc. Natl. Acad. Sci. U. S. A.* **1997**, *94*, 13390.
- (9) Nissen, J.; Gritsch, S.; Wiegand, G.; Rädler, J. O. *Eur. Phys. J. B.* **1999**, *10*, 335.
- (10) Hovis, J. S.; Boxer, S. G. *Langmuir* **2000**, *16*, 894.
- (11) Cho, N.-J.; Frank, C. W. *Langmuir* **2010**, *26*, 15706.
- (12) Daniel, S.; Diaz, A. J.; Martinez, K. M.; Bench, B. J.; Albertorio, F.; Cremer, P. S. *J. Am. Chem. Soc.* **2007**, *129*, 8072.
- (13) Jönsson, P.; Beech, J. P.; Tegenfeldt, J. O.; Höök, F. *J. Am. Chem. Soc.* **2009**, *131*, 5294.
- (14) Liu, C.; Monson, C. F.; Yang, T.; Pace, H.; Cremer, P. S. *Anal. Chem.* **2011**, *83*, 7876.

- (15) White, R. J.; Ervin, E. N.; Yang, T.; Chen, X.; Daniel, S.; Cremer, P. S.; White, H. S. *J. Am. Chem. Soc.* **2007**, *129*, 11766.
- (16) Poo, M. M.; Robinson, K. R. *Nature* **1977**, *265*, 602.
- (17) Groves, J. T.; Boxer, S. G. *Biophys. J.* **1995**, *69*, 1972.
- (18) Groves, J. T.; Wulfing, C.; Boxer, S. G. *Biophys. J.* **1996**, *71*, 2716.
- (19) Cheetham, M. R.; Bramble, J. P.; McMillan, D. G. G.; Krzeminski, L.; Han, X.; Johnson, B. R. G.; Bushby, R. J.; Olmsted, P. D.; Jeuken, L. J. C.; Marritt, S. J.; Butt, J. N.; Evans, S. D. *J. Am. Chem. Soc.* **2011**, *133*, 6521.
- (20) McLaughlin, S.; Poo, M. M. *Biophys. J.* **1981**, *34*, 85.
- (21) Cremer, P. S.; Groves, J. T.; Kung, L. A.; Boxer, S. G. *Langmuir* **1999**, *15*, 3893.
- (22) Groves, J. T.; Boxer, S. G. *Accounts Chem. Res.* **2002**, *35*, 149.
- (23) Jackson, B. L.; Groves, J. T. *J. Am. Chem. Soc.* **2004**, *126*, 13878.
- (24) Kam, L.; Boxer, S. G. *Langmuir* **2003**, *19*, 1624.
- (25) Kung, L. A.; Kam, L.; Hovis, J. S.; Boxer, S. G. *Langmuir* **2000**, *16*, 6773.
- (26) Shi, J.; Chen, J.; Cremer, P. S. *J. Am. Chem. Soc.* **2008**, *130*, 2718.
- (27) Shi, J.; Yang, T.; Cremer, P. S. *Anal. Chem.* **2008**, *80*, 6078.
- (28) Yee, C. K.; Amweg, M. L.; Parikh, A. N. *J. Am. Chem. Soc.* **2004**, *126*, 13962.
- (29) Monson, C. F.; Pace, H.; Liu, C.; Cremer, P. S. *Anal. Chem.* **2011**, *83*, 2090.
- (30) Cristea, I. M.; Gaskell, S. J.; Whetton, A. D. *Blood* **2004**, *103*, 3624.
- (31) Phizicky, E.; Bastiaens, P. I. H.; Zhu, H.; Snyder, M.; Fields, S. *Nature* **2003**, *422*, 208.
- (32) Zheng, H. A.; Zhao, J.; Sheng, W. Y.; Xie, X. Q. *Biopolymers* **2006**, *83*, 46.

- (33) Zhu, H.; Bilgin, M.; Bangham, R.; Hall, D.; Casamayor, A.; Bertone, P.; Lan, N.; Jansen, R.; Bidlingmaier, S.; Houfek, T.; Mitchell, T.; Miller, P.; Dean, R. A.; Gerstein, M.; Snyder, M. *Science* **2001**, *293*, 2101.
- (34) Nabika, H.; Sasaki, A.; Takimoto, B.; Sawai, Y.; He, S.; Murakoshi, K. *J. Am. Chem. Soc.* **2005**, *127*, 16786.
- (35) Neumann, J.; Hennig, M.; Wixforth, A.; Manus, S.; Rädler, J. O.; Schneider, M. *F. Nano Lett.* **2010**, *10*, 2903.
- (36) Stelzle, M.; Miehlisch, R.; Sackmann, E. *Biophys. J.* **1992**, *63*, 1346.
- (37) van Oudenaarden, A.; Boxer, S. G. *Science* **1999**, *285*, 1046.
- (38) Yoshina-Ishii, C.; Boxer, S. G. *Langmuir* **2006**, *22*, 2384.
- (39) Han, X. J.; Cheetham, M. R.; Sheikh, K.; Olmsted, P. D.; Bushby, R. J.; Evans, S. D. *Integr. Biol.* **2009**, *1*, 205.
- (40) Nelson, D. L.; Cox, M. M. *Lehninger Principles of Biochemistry*; 3rd ed.; Worth Publishers: New York, 2000.
- (41) Lou, C.; Shindel, M.; Graham, L.; Wang, S.-W. *Langmuir* **2008**, *24*, 8111.
- (42) Ratanabanangkoon, P.; Gast, A. P. *Langmuir* **2002**, *19*, 1794.
- (43) Prin, C.; Bene, M. C.; Gobert, B.; Montagne, P.; Faure, G. C. *Biochim. Biophys. Acta-Gen. Subj.* **1995**, *1243*, 287.
- (44) Sivasankar, S.; Subramaniam, S.; Leckband, D. *Proc. Natl. Acad. Sci. U. S. A.* **1998**, *95*, 12961.
- (45) Schneider, S. W.; Lärmer, J.; Henderson, R. M.; Oberleithner, H. *Pflüg. Arch. Eur. J. Phy.* **1998**, *435*, 362.

- (46) Yan, H.; Park, S. H.; Finkelstein, G.; Reif, J. H.; LaBean, T. H. *Science* **2003**, *301*, 1882.
- (47) Shaw, D. J. *Introduction to Colloid and Surface Chemistry*; 3rd ed.; Butterworth & Co Ltd: UK, 1980.
- (48) Poger, D.; Mark, A. E. *J. Chem. Theory Comput.* **2010**, *6*, 325.
- (49) Behrens, S. H.; Grier, D. G. *J. Chem. Phys.* **2001**, *115*, 6716.
- (50) Castellana, E. T.; Cremer, P. S. *Surf. Sci. Rep.* **2006**, *61*, 429.
- (51) Tanaka, M.; Sackmann, E. *Nature* **2005**, *437*, 656.
- (52) Du, H.; Ren, J.; Wang, S.; He, L. *Anal. Bioanal. Chem.* **2011**, *400*, 3625.
- (53) Cook, A. C.; Ho, C.; Kershner, J. L.; Malinowski, S. A.; Moldveen, H.; Stagliano, B. A.; Slater, S. J. *Biochemistry* **2006**, *45*, 14452.
- (54) Mai, A.; Veltel, S.; Pellinen, T.; Padzik, A.; Coffey, E.; Marjomäki, V.; Ivaska, J. *J. Cell Biol.* **2011**, *194*, 291.
- (55) Wu, Z. C.; de Keyzer, J.; Kedrov, A.; Driessen, A. J. *J. Biol. Chem.* **2012**, *287*, 7885.
- (56) Baksh, M. M.; Kussrow, A. K.; Mileni, M.; Finn, M. G.; Bornhop, D. J. *Nat. Biotechnol.* **2011**, *29*, 357.
- (57) Stites, W. E. *Chem. Rev.* **1997**, *97*, 1233.
- (58) Li, J.; Swanson, R. V.; Simon, M. I.; Weis, R. M. *Biochemistry* **1995**, *34*, 14626.
- (59) Stock, A. M.; Robinson, V. L.; Goudreau, P. N. *Annu. Rev. Biochem.* **2000**, *69*, 183.
- (60) Arlett, J. L.; Myers, E. B.; Roukes, M. L. *Nat. Nanotechnol.* **2011**, *6*, 203.

- (61) Armani, A. M.; Kulkarni, R. P.; Fraser, S. E.; Flagan, R. C.; Vahala, K. J. *Science* **2007**, *317*, 783.
- (62) Jung, H.; Robison, A. D.; Cremer, P. S. *J. Am. Chem. Soc.* **2009**, *131*, 1006.
- (63) Ray, S.; Mehta, G.; Srivastava, S. *Proteomics* **2010**, *10*, 731.
- (64) Ray, S.; Reddy, P. J.; Jain, R.; Gollapalli, K.; Moiyadi, A.; Srivastava, S. *Proteomics* **2011**, *11*, 2139.
- (65) Vollmer, F.; Arnold, S. *Nat. Meth.* **2008**, *5*, 591.
- (66) Yu, X.; Xu, D.; Cheng, Q. *Proteomics* **2006**, *6*, 5493.
- (67) Cooper, M. A.; Dultsev, F. N.; Minson, T.; Ostanin, V. P.; Abell, C.; Klenerman, D. *Nat. Biotechnol.* **2001**, *19*, 833.
- (68) Nam, J.-M.; Thaxton, C. S.; Mirkin, C. A. *Science* **2003**, *301*, 1884.
- (69) Wang, W. U.; Chen, C.; Lin, K.-h.; Fang, Y.; Lieber, C. M. *Proc. Natl. Acad. Sci. U. S. A.* **2005**, *102*, 3208.
- (70) Shi, J.; Yang, T.; Cremer, P. S. *Anal. Chem.* **2008**, *80*, 6078.
- (71) Prin, C.; Bene, M. C.; Gobert, B.; Montagne, P.; Faure, G. C. *Biochim. Biophys. Acta, Gen. Subj.* **1995**, *1243*, 287.
- (72) Stace, C. L.; Ktistakis, N. T. *Biochim. Biophys. Acta-Mol. Cell. Biol. L.* **2006**, *1761*, 913.
- (73) Verhoven, B.; Schlegel, R. A.; Williamson, P. J. *Exp. Med.* **1995**, *182*, 1597.
- (74) Haucke, V.; Di Paolo, G. *Curr. Opin. Cell Biol.* **2007**, *19*, 426.
- (75) Wymann, M. P.; Schneider, R. *Nat. Rev. Mol. Cell Biol.* **2008**, *9*, 162.
- (76) Athenstaedt, K.; Daum, G. *Eur. J. Biochem.* **1999**, *266*, 1.



- (77) Voelker, D. R. *Microbiol. Rev.* **1991**, *55*, 543.
- (78) Wang, X.; Devaiah, S. P.; Zhang, W.; Welti, R. *Prog. Lipid Res.* **2006**, *45*, 250.
- (79) Hancock, J. F. *Nat. Cell Biol.* **2007**, *9*, 615.
- (80) Selvy, P. E.; Lavieri, R. R.; Lindsley, C. W.; Brown, H. A. *Chem. Rev.* **2011**, *111*, 6064.
- (81) Swairjo, M. A.; Seaton, B. A.; Roberts, M. F. *Biochim. Biophys. Acta - Biomembranes* **1994**, *1191*, 354.
- (82) Kooijman, E. E.; Chupin, V.; de Kruijff, B.; Burger, K. N. J. *Traffic* **2003**, *4*, 162.
- (83) Bi, K.; Roth, M. G.; Ktistakis, N. T. *Curr. Biol.* **1997**, *7*, 301.
- (84) Imamura, S.; Horiuti, Y. *J. Biochem.* **1979**, *85*, 79.
- (85) Yamamoto, I.; Konto, A.; Handa, T. *Biochim. Biophys. Acta - Biomembranes* **1995**, *1233*, 21.
- (86) Holbrook, P. G.; Pannell, L. K.; Daly, J. W. *Biochim. Biophys. Acta - Lipid. Lipid Met.* **1991**, *1084*, 155.
- (87) El Kirat, K.; Duprès, V.; Dufrêne, Y. F. *Biochim. Biophys. Acta - Biomembranes* **2008**, *1778*, 276.
- (88) Brown, H. A.; Sternweis, P. C. *Methods Enzymol.* **1995**, *257*, 313.
- (89) M, T.; S, I.; T, N.; I, T. *Clin. Chim. Acta* **1977**, *79*, 93.
- (90) Morishita, Y.; Inuma, Y.; Nakashima, N.; Kadota, A.; Miike, A.; Tadano, T. *Clin. Chem.* **1999**, *45*, 2280.
- (91) Chalifa, V.; Möhn, H.; Liscovitch, M. *J. Biol. Chem.* **1990**, *265*, 17512.

- (92) Liu, C.; Monson, C. F.; Yang, T.; Pace, H.; Cremer, P. S. *Anal. Chem.* **2011**, *83*, 7876.
- (93) Hovis, J. S.; Boxer, S. G. *Langmuir* **2001**, *17*, 3400.
- (94) Kam, L.; Boxer, S. G. *J. Am. Chem. Soc.* **2000**, *122*, 12901.
- (95) Smith, K. A.; Gale, B. K.; Conboy, J. C. *Anal. Chem.* **2008**, *80*, 7980.

## VITA

Name: Chunming Liu  
Address: No. 83, Jingsan Lu, Jinan, Shandong, 250001, China  
Email Address: [chunming@mail.chem.tamu.edu](mailto:chunming@mail.chem.tamu.edu)  
Phone number: (979) – 739 – 1565  
Education: B.S., Chemistry, Nanjing University, 2007